



Calhoun: The NPS Institutional Archive DSpace Repository

Theses and Dissertations

1. Thesis and Dissertation Collection, all items

1966

The infrared spectra of formaldehyde and formaldehyde-d₂

Hoyes, Donald J.

<http://hdl.handle.net/10945/9537>

This publication is a work of the U.S. Government as defined in Title 17, United States Code, Section 101. Copyright protection is not available for this work in the United States.

Downloaded from NPS Archive: Calhoun



<http://www.nps.edu/library>

Calhoun is the Naval Postgraduate School's public access digital repository for research materials and institutional publications created by the NPS community.

Calhoun is named for Professor of Mathematics Guy K. Calhoun, NPS's first appointed -- and published -- scholarly author.

Dudley Knox Library / Naval Postgraduate School
411 Dyer Road / 1 University Circle
Monterey, California USA 93943

NPS ARCHIVE

1966

HOYES, D.

THE INFRARED SPECTRA OF FORMALDEHYDE
AND FORMALDEHYDE-d₂.

DONALD J. HOYES

L7-17
Naval Postgraduate School
Monterey, California

DUDLEY KNOX LIBRARY
NAVAL POSTGRADUATE SCHOOL
MONTEREY CA 93943-5101



Nov 196

DUDLEY KNOX LIBRARY
NAVAL POSTGRADUATE SCHOOL
MONTEREY CA 93943-5101

THE INFRARED SPECTRA
OF
FORMALDEHYDE AND FORMALDEHYDE-d₂

LCDR Donald J. Hoyes, U.S. Navy

//

A Thesis

in

Chemistry

Presented to the Faculty of the Graduate School
of Arts and Sciences of the University of
Pennsylvania in Partial Fulfillment
of the Requirements for the Degree
of Master of Science

1966

Index

Angular Momentum, 14
Asymmetric Top Molecules, 3, 11, 23, 71
Band Contour 11, 14-16, 23
Band Types 24, 25
Centrifugal Stretching, 13
Combination Bands, 11, 30
Coriolis Coupling 19-22, 53, 59, 60
Coriolis Force 20
Crystals 29, 30, 41, 43, 50
 Infrared Spectra of 46, 47, 80
Degenerate Vibrations 30, 43
Degrees of Freedom
 Vibrational 9
Dipole Moment 11
Excited States 16, 33
Fermi Resonance 22, 23, 49, 53, 57, 59
Formaldehyde (Gaseous)
 Conclusion 40
 Discussion of Spectrum 34 - 39
 Impurities in 33, 34
 Molecular Structure 31
 Preparation 33, 34
 Previous Studies 31, 32
 Rotational Analysis 33, 38
 Spectrum 32, 35, 37

Formaldehyde (Solid)

Conclusion 52
Crystal Splitting in 41, 43, 50, 52
Discussion of Spectrum 45, 51
Fermi Resonance in 49, 50
Preparation 44, 45
Spectrum 46, 47, 48
Unit Cell 42, 52

Formaldehyde-d₂ (Gaseous)

Conclusion 72
Coriolis Interactions of 53, 59
Discussion of Spectrum 54, 59, 60
Fermi Resonance in 53, 57, 59, 60
Molecular Structure of 53
Preparation 54
Rotational Analysis 53, 76
Spectrum 55, 56, 61, 62, 64, 70
Teller-Redlich Product Rule 57

Formaldehyde-d₂ (Solid)

Conclusion 82
Discussion of Spectrum 79
Impurities in 79
Preparation 78
Spectrum 80, 81
Teller-Redlich Product Rule 79, 80

Fundamental Vibrations 11

Inertia Defect 32

Isotopic Substitution 27, 45

Linear Molecule 18, 24

Moments of Inertia 3, 4

Normal Coordinates 9

Normal Vibrations 9, 10

Oblate Symmetric Top 24
Overtone Bands 11
Parallel Bands 12, 14, 17
Perpendicular Bands 18
Planar Molecules 23, 24, 32
Point Group 7, 8
Principal axes 3
Prolate Symmetric Top 4, 24
Relative Intensity of P, Q, and R branches 18
Rotational Constants 13, 16, 19, 26, 53, 76
Rotational Energy 13
Selection Rules 12, 17, 18
Symmetry Species 9, 28
Symmetric Top Molecules 4, 5, 11
Symmetry Elements and Operations 5
Teller-Redlich Product Rule 27, 28, 29, 57, 79
Unit cell 42
Vibration-Rotation Interactions 16, 19

Table of Contents

INDEX	ii	
TABLE OF CONTENTS	v	
LIST OF TABLES	vi	
LIST OF ILLUSTRATIONS	viii	
BIBLIOGRAPHY	x	
PREFACE	xii	
I.	Abstract	1
	Symmetric Top Molecules	2
	Symmetry	4
	Band Contours	11
	Isotopic Substitution	27
	Solid States	29
II.	Gaseous Formaldehyde	
	Introduction	31
	Experimental	33
	Discussion	34
	Conclusion	40
III.	Polycrystalline Formaldehyde	
	Introduction	41
	Experimental	44
	Discussion	45
	Conclusion	52
IV.	Gaseous Formaldehyde-d ₂	
	Introduction	53
	Experimental	54
	Discussion	54
	Conclusion	72
V.	Polycrystalline Formaldehyde-d ₂	
	Introduction	78
	Experimental	78
	Discussion	79
	Conclusion	82

List of Tables

Table		Page
I	The Symmetry Elements and Symmetry of Operations	5
II	Some of the Point Groups That Are Important in Molecular Problems	7
III	Frequencies (cm^{-1}) of the P, Q, and R Branches of $2\nu_2$ of Gaseous Formaldehyde	37
IV	A Comparison of the Band Centers (cm^{-1}) of Polycrystalline and Gaseous Formaldehyde	48
V	Infrared Band Centers (cm^{-1}) of Gaseous Formaldehyde	56
VI	A Comparison of the Calculated and Observed Teller-Redlich Product Rule Ratios for $D_2\text{CO}$ and $H_2\text{CO}$ Gases	58
VII	Frequencies (cm^{-1}) of the Fundamental Vibration ν_1 ($D_2\text{CO}$ Gas)	64
VIII	Frequencies (cm^{-1}) of the Fundamental Vibration ν_2 ($D_2\text{CO}$ Gas)	65
IX	Frequencies (cm^{-1}) of the Fundamental Vibration ν_3 ($D_2\text{CO}$ Gas)	66
X	Frequencies (cm^{-1}) of the Fundamental Vibration ν_4 ($D_2\text{CO}$ Gas)	67
XI	Frequencies (cm^{-1}) of the Fundamental Vibration ν_5 ($D_2\text{CO}$ Gas)	69

XII	Frequencies (cm^{-1}) of the Fundamental Vibration ν_6 (D_2CO Gas)	70
XIII	Rotational Combination Constants for the Ground and First Excited States of Gaseous D_2CO	76
XIV	Band Centers (cm^{-1}), Frequency Shifts (cm^{-1}), and Assignments of the Infrared Spectrum of Polycrystalline D_2CO	81
XV	A Comparison of the Calculated and Observed Teller-Redlich Product Rule Ratios for Polycrystalline D_2CO and H_2CO	83

List of Illustrations

Figure		Page
1	The C_{2v} Symmetry of $H_2CO(D_2CO)$	8
2	The Normal Vibrations of H_2CO and D_2CO	10
3	The Rotational Energy-Level Patterns for Symmetric-Top Molecules	15
4	The Components of a Parallel Band	17
5	Coriolis Forces in Linear XY_2	21
6	Typical A, B, and C Type Band Contours	25
7	Survey and High Resolution Spectra of Gaseous H_2CO	35
8	Graph of Equation (17) Applied to $2\nu_2$ of Gaseous H_2CO	38
9	Infrared Spectra of Polycrystalline H_2CO at $-190^\circ C$.	46
10	Infrared Spectra of Polycrystalline (A) Pure H_2CO , (B) 15% H_2CO , and (C) 1% H_2CO in D_2CO at $-190^\circ C$	47
11	Infrared Spectrum of Gaseous DCDO	55
12	Infrared High Resolution Spectra of ν_1 , ν_2 and ν_3 of Gaseous DCDO	61
13	Infrared High Resolution Spectra of ν_4 , ν_5 and ν_6 of Gaseous DCDO	62
14	Graph of Equation (22) Applied to ν_1 of Gaseous D_2CO	73

15	Graph of Equation (22) Applied to ν_2 of Gaseous D ₂ CO	74
16	Graph of Equation (22) Applied to ν_3 of Gaseous D ₂ CO	75
17	Infrared Spectrum of Polycrystalline D ₂ CO at -190°C	80

Bibliography

(The numbers correspond to pages in the text.)

- Barrow, G., Molecular Spectroscopy, McGraw-Hill
Book Company, Inc., 1962. 5, 6
- Bernstein, H.J., and Schneider, W.G., Trans. Faraday
Soc., 52, 13 (1956) 36, 41
- Blau, H.H., and Nielsen, H.H., J. Mol. Spectroscopy,
1, 124 (1957). 4, 20, 22, 23, 31
36, 39, 49, 59, 72
- Cleveland, F.F., and Pillai, M.G.K. J. Mol.
Spectroscopy, 6, 465 (1961). 32, 54
- Davidson, D.W., Stoicheff, B.P., and Bernstein, H.J.
J. Chem. Phys., 22, No. 2, 289 (1954). 79
- Ebers, E.S., and Nielsen, H.H., J. Chem. Phys., 6
311 (1938). 4, 53, 54
- Harvey, K.B., and Ogilvie, J.F. Can. J. Chem. 40,
85 (1962) 36
- Herzberg, G., Infrared and Raman Spectra, D. Van
Nostrand Company, Inc., Princeton, N.J. 1945 6, 27, 59, 60
- Morino, Y. and Oka, T., J. Mol. Spectroscopy, 11,
349 (1965). 32
- Morino, Y., Oka, T., and Takagi, K., J. Mol.
Spectroscopy, 14, 27 (1964). 31
- Oka, T., J. Phys. Soc. Japan, 15, No. 12, 2274 (1960). 3, 24, 31, 32
39, 53, 72

- Oka, T. and Takagi, K., J. Phys. Soc. Japan,
18, No. 8, 1174 (1963). 31, 53
- Oka, T. Hirakawa, H., and Shimoda, K., J. Phys.
Soc. Japan, 15, No. 12, 2265 (1960). 31
- Shimanouchi, T., and Suzuki, I., J. Chem. Phys.,
42, No. 1, 296 (1965). 32
- Tadokoro, H., et al, J. Chem. Phys., 38, No. 3,
703 (1963). 34
- Walker, J. F., Formaldehyde, Reinhold Publishing
Corporation, N. Y. (1953) 33

Preface

The author wishes to express his sincere appreciation to Dr. Eugene R. Nixon for his very helpful suggestions and guidance during the course of this investigation.

The author is also indebted to the Office of Naval Research for financial aid extended during the period from 1964 - 1965.

The Infrared Spectrum of Formaldehyde
and Formaldehyde-d₂.

Abstract

The infrared spectra of solid and gaseous H₂CO and D₂CO were examined in the range from 4000 to 500 cm⁻¹. The previously unreported 2ν₂ overtone band of gaseous H₂CO was observed and the rotational constants (B' + C') for that excited state were evaluated. The spectrum of solid D₂CO is reported for the first time.

Many new assignments have been made for D₂CO gas. Examples of Fermi resonance between ν₁ and 2ν₅ and Coriolis resonance interactions among ν₃, ν₅ and ν₆ were noted. Certain combinations of the ground state and first excited state rotational constants were evaluated for ν₁, ν₂, ν₃, ν₄ and ν₅.

Using the Teller-Redlich product rule, the six fundamental frequencies of solid D₂CO were assigned. Several combination and overtone bands were also assigned.

Using isolation techniques, factor group crystal splitting was detected in solid H₂CO. This leads to the conclusion that solid H₂CO has at least two molecules per unit cell.

I. Introduction: Symmetric Top Molecules

The classification of molecules with respect to their vibration-rotation spectra depends upon the moments of inertia about the principal axes of the molecule.

The principal axes of a molecule are defined as that set of three mutually perpendicular axes which pass through the center of gravity of the molecule and for which one of the axes corresponds to the least moment of inertia (I_A), and one axis corresponds to the largest moment of inertia (I_C). The moment about the third axis has an intermediate value, I_B .

A moment of inertia of a system of masses m_i about any particular axis is given by the relation

$$I = \sum_i m_i x_i^2 \quad (1)$$

where x_i is the perpendicular distance of the particle of mass m_i , from the axis.

If, for a molecule, all three principal moments of inertia are different ($I_A \neq I_B \neq I_C$), the molecule is called an asymmetric top. Most molecules fall into this category.

A molecule which has just two equal principal moments of inertia and the third moment non-vanishing ($I_A < I_B = I_C$ for example), is termed a symmetric top molecule.

If $I_A < I_B = I_C$, the molecule is called a prolate symmetric top. On the other hand, the molecule that has $I_A = I_B < I_C$ is called an oblate symmetric top.

Many molecules, although actually asymmetric tops, may be treated as if they are symmetric tops if two of their principal moments of inertia are almost equal.

This is the case of H_2CO and D_2CO where the following principal moments of inertia have been determined from microwave spectra:¹

<u>H_2CO (amu \AA^2)</u>	<u>D_2CO (amu \AA^2)</u>
I_A 1.81517	I_A 3.60483
I_B 13.07375	I_B 15.7239
I_C 14.89022	I_C 19.3286

It will be noted that for both H_2CO and D_2CO , $I_A < I_B \approx I_C$ which means that both molecules are close to prolate symmetric tops.

Because of the closeness of both H_2CO and D_2CO to symmetric

¹T. Oka, J. of the Physical Soc. of Japan, 15, No. 12, 2274 (1960).

tops and the complexity involved in handling asymmetric top molecules, all previous infrared work,^{2, 3} including the present one, have treated these molecules as symmetric tops.

Symmetry

The use of symmetry in spectroscopy is very important since symmetry considerations may simplify the complex problems of the vibrations and rotations of molecules.

By the term symmetry we mean the symmetry of the equilibrium arrangement of the atomic nuclei of the molecules. In general, molecules of different symmetry exhibit qualitatively different spectra. Consequently, qualitative conclusions regarding the equilibrium geometry of the molecule, such as whether the molecule is linear or planar, may be drawn from the spectra.

In order to discuss the symmetry of H₂CO and D₂CO, it is necessary first to describe the terms used in symmetry.

The symmetry of a molecule may be described in terms of five possible symmetry elements and their corresponding symmetry operations. (Table I).⁴ The more symmetric a molecule, the more

²E. S. Ebers, and H. H. Nielsen, J. Chem. Phys., 6, 311 (1938)

³H. H. Blau and H. H. Nielsen, J. Mol. Spectroscopy, 1, 124 (1957)

⁴G. Barrow, Molecular Spectroscopy, McGraw-Hill Book Company, Inc. 1962. p. 160.

Table 1. The Symmetry Elements
and Symmetry Operations.

Symmetry Elements		Symmetry Operations
Symbol	Description	
E	Identity	No change
σ	Plane of symmetry	Reflection through the plane
i	Center of symmetry	Inversion through the center
C_p	'Axis of symmetry'	Rotation about the axis by 360/p degrees
S	Rotation-reflection axis of symmetry	Rotation about the axis by 360/p degrees followed by reflection through the plane.

(From Barrow, p. 160)

symmetry elements it possesses. Each combination of symmetry elements that can occur is known as a point group. The term point group is used because the symmetry operators that are associated with the symmetry elements of the molecule leaves a point of the molecule fixed in space.

A summary of the more common point groups and the symbols used to denote them are given in Table II.⁵ In the point group symbol, the capital letter denotes, in general, the principal symmetry element of the group while the subscripts further tie in the relationship to the other symmetry elements of the group.

Formaldehyde and Formaldehyde-d₂ belong to point group C_{2v}, which consists of a two-fold axis C₂ and two planes of symmetry σ_v through the axis. The symbol v indicates vertical planes of symmetry and the two-fold axis refers to a rotation of 180° about the axis. In the case of H₂CO and D₂CO the two vertical planes of symmetry, σ_v and σ'_v and the two-fold axis C₂ are shown in Figure 1.

From a knowledge of the point group, the irreducible representations can be found from suitable references.⁶

⁵Ibid. p. 161

⁶G. Herzberg, Infrared and Raman Spectra, D. Van Nostrand Co., Inc., Princeton, N.J. (1949).

Table II. Some of the Point Groups
That Are Important in Molecular Problems

(The number of times a symmetry element occurs is indicated by a number before the symbol for that symmetry element)

Point group	Symmetry elements	Examples
C_1	E	$\text{CH}_3-\text{CHClBr}$
C_5	E,	NOCl , CH_3OSiH_3
C_{2v}	E, C_2 , $2\sigma_v$	H_2O , CH_2Cl_2
C_{3v}	E, C_3 , $3\sigma_v$	NH_3 , HCCl_3
$C_{\infty v}$	E, C_{∞} , $\omega\sigma_v$	HCN , OCS
C_{2h}	E, C_2 , σ_h , i	$\text{ClHC}=\text{CHCl}$ (trans.)
D_{3d}	E, C_3 , $3C_2$ (perp. to the C_3 axis), S_6 (coincident with the C_3 axis), i, $3\sigma_d$	C_6H_{12} (cyclohexane)
$D_{2h} \equiv V_h$	E, $3C_2$ (mutually perp.), 3σ (mutually perp.), i	$\text{H}_2\text{C}=\text{CH}_2$
D_{3h}	E, C_3 , $3C_2$ (perp. to the C_3 axis), $3\sigma_v$, σ_h	BCl_3
D_{4h}	E, C_4 , $4C_2$ (perp. to the C_4 axis), $4\sigma_v$, $4\sigma_h$, C_2 and S_4 (both coincident with C_4), i	C_4H_8 (cyclobutane)
D_{6h}	E, C_6 , $6C_2$ (perp. to the C_6 axis), $6\sigma_v$, σ_h , C_2 and C_3 and S_6 (all coincident with the C_6 axis), I	C_6H_6 (benzene)
$D_{\infty h}$	E, C_{∞} , ωC_2 (perp. to the C_{∞} axis), σ_v , σ_h , i	H_2 , CO_2 , $\text{HO}=\text{CH}$
T_d	E, $3C_2$ (mutually perp.), $4C_3$, CH_4 , 6σ , $3S_4$ (coincident with the C_2 axes),	
O_h	E, $3C_4$ (mutually perp.), $4C_3$, $(\text{PtCl}_6)^=$, $3S_4$ and $3C_2$ (coincident with the C_4 axes), $6C_2$, 9σ , $(\text{Co}(\text{NH}_3)_6)^{3+}$, $4S_6$ (coincident with the C_3), i	

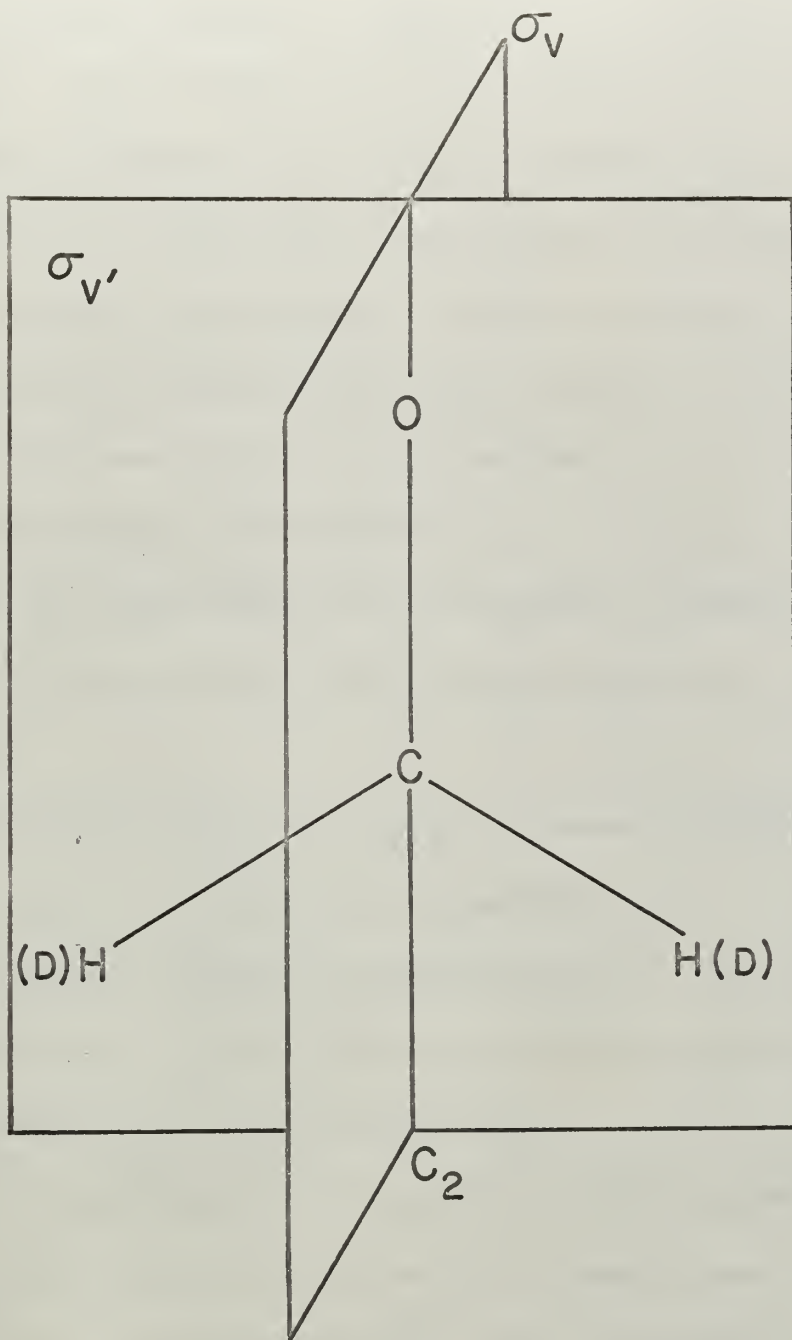


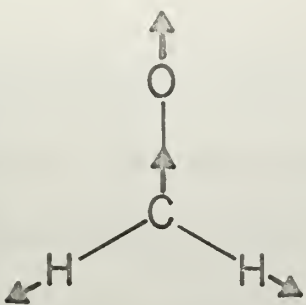
Figure 1. The C_{2v} symmetry of H_2CO (D_2CO).

A non-linear molecule composed of N atoms has $3N-6$ normal vibrations. Normal vibrations are immediately related to a set of convenient coordinates called normal coordinates which are especially convenient for the description of the vibrations of a system. Each normal coordinate corresponds to a mode of vibrations in which every atom of the molecule carries out a simple harmonic motion and all atoms have exactly the same frequency and phase of oscillation. Only the amplitudes of vibration may vary from atom to atom. Thus, motion of the system along a normal coordinate consists of simple harmonic motion, and such motion is said to be a normal mode or vibration.

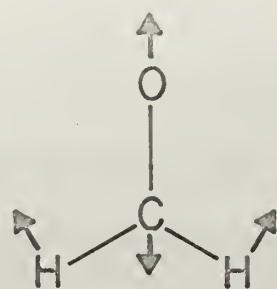
In the case of H_2CO and D_2CO , the normal vibrations are as shown in Figure 2. Knowing the normal vibrations, it is possible to assign each to a symmetry species for the C_{2v} point group. It turns out that ν_1 , ν_2 and ν_3 belong to symmetry species A_1 , ν_4 and ν_5 belong to B_1 , and ν_6 belongs to B_2 .

It is interesting to note that all six normal vibrations of H_2CO and D_2CO are infrared active since only symmetry species A_2 of point group C_{2v} is infrared inactive. This is due to the fact that there is no dipole moment change for A_2 vibrations.

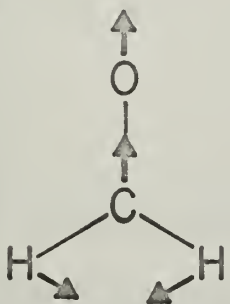
Those vibrations which correspond to a change in the vibrational



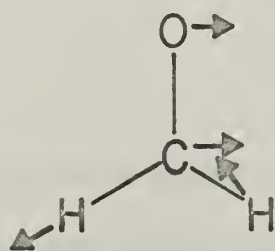
ν_1 (symmetric CH stretch)



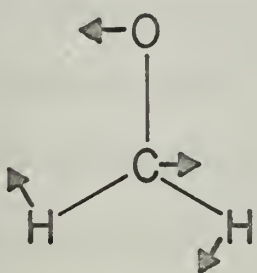
ν_2 (CO stretch)



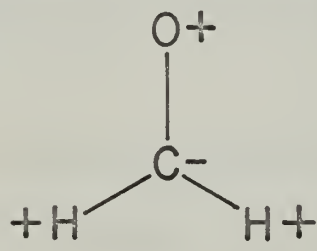
ν_3 (CH₂ bending)



ν_4 (asymmetric CH stretch)



ν_5 (CH₂ rocking)



ν_6 (CH₂ wagging)

Figure 2. The normal vibrations of H₂CO and D₂CO. (From G. Herzberg, p. 65).

quantum number $\nu = 0$ to $\nu = 1$ are called fundamental vibrations.

Since the ground vibrational state ($\nu = 0$) is usually the most densely populated, the fundamentals usually appear as the most intense bands of the infrared spectrum. In addition, overtone ($\Delta\nu_i > 1$) and combination (simultaneous changes in two or more ν_i) bands may appear, but these are usually of much lower intensity.

Band Contours

As previously discussed, H_2CO and D_2CO are slightly asymmetric tops but they are so close to a symmetric top that both molecules may be described in terms of a symmetric top. Therefore, the predicted shapes of the infrared absorption bands will now be discussed in terms of the symmetric top and then compared with the band shapes expected for asymmetric tops.

To be optically active in the infrared, a given vibration-rotation transition must result in a non-zero transition moment. The exact rotational selection rules depend upon the direction of that dipole moment change.

The infrared active normal vibrations (ν_1, ν_2 , etc.) of symmetric top molecules have their oscillating dipole moment either parallel or perpendicular to the "unique" axis of the molecule. The unique axis of the molecule is that axis which

corresponds to the unique moment of inertia of the molecule. For example, H_2CO and D_2CO are approximately prolate symmetric tops and therefore I_A is the unique axis ($I_A < I_B = I_C$).

These two different types of vibrations thus have different vibration-rotation selection rules and as a result exhibit different band shapes.

An oscillating dipole moment parallel to the unique axes of the molecule gives rise to a parallel band. For such vibrations, the selection rules are:

$$\Delta K = 0, \Delta J = \pm 1 \quad \text{if } K = 0 \tag{2}$$

$$\Delta K = 0, \Delta J = 0, \pm 1 \text{ if } K \neq 0 \tag{3}$$

where J is the rotational quantum number for the total angular momentum, with values of 0, 1, 2,

K is the rotational quantum number for the component of the total angular momentum about the unique axis, with values of 0, $\pm 1, \pm 2, \dots J$.

The reason for the selection rule $\Delta K=0$ in a parallel band lies in the fact that rotation about the unique axis cannot result in any interaction with radiation since such a rotation does not result in any dipole moment change. Radiant energy, therefore, cannot produce a transition between levels of different K values.

At this point, it would be well to give the expression for the rotational energies of a symmetric top molecule, assuming a rigid rotor model.

$$E_{J,k} = B J (J+1) + (A - B) K^2 \quad (4)$$

where A and B are the rotational constants and related to the principal moments of inertia by:

$$A = \frac{h^2}{8\pi^2 C I_A} \quad (5)$$

$$B = \frac{h^2}{8\pi^2 C I_B}$$

where I_A is the principal moment of inertia about the unique axis.

I_B is the principal moment of inertia about either of the other principal axes.

h is Planck's constant (6.625×10^{-27} erg-sec)

C is the velocity of light in a vacuum (2.998×10^{10} cm/sec.)

In cases in which the rigid rotor model for a molecule is not adequate, correction terms may be added to (4) to account for centrifugal stretching.

Except in those cases where extremely accurate measurements are required, these additional terms are negligible.

The transitions that constitute the parallel band of a symmetric top molecule follow from equations (2) (3), and (4) and can be represented on the energy diagram of Figure 3. The absorption spectrum consists of a set of evenly spaced lines with a separation of $2B$. Thus, the rotational line spacing yields the moment of inertia, I_B .

The band contour of a parallel band depends upon the selection rules shown in equations (2) and (3). For each transition between different J values of a given K value, a characteristic absorption pattern results. If $K = 0$, then according to equation (2), $\Delta J = \pm 1$. This subband then has two branches, one corresponding to $\Delta J = +1$ and the other corresponding to $\Delta J = -1$. These are designated as R and P branches respectively. For $K \neq 0$, $\Delta J = 0, \pm 1$, then each of the rest of the subbands corresponding to $K = 1, 2, 3, \dots$ will have $\Delta J = 0$ in addition to the P and R branches. This transition results in a very strong central peak which is designated as the Q branch.

Since K determines a component of the angular momentum while J determines the total angular momentum, J must always be equal to or greater than K .

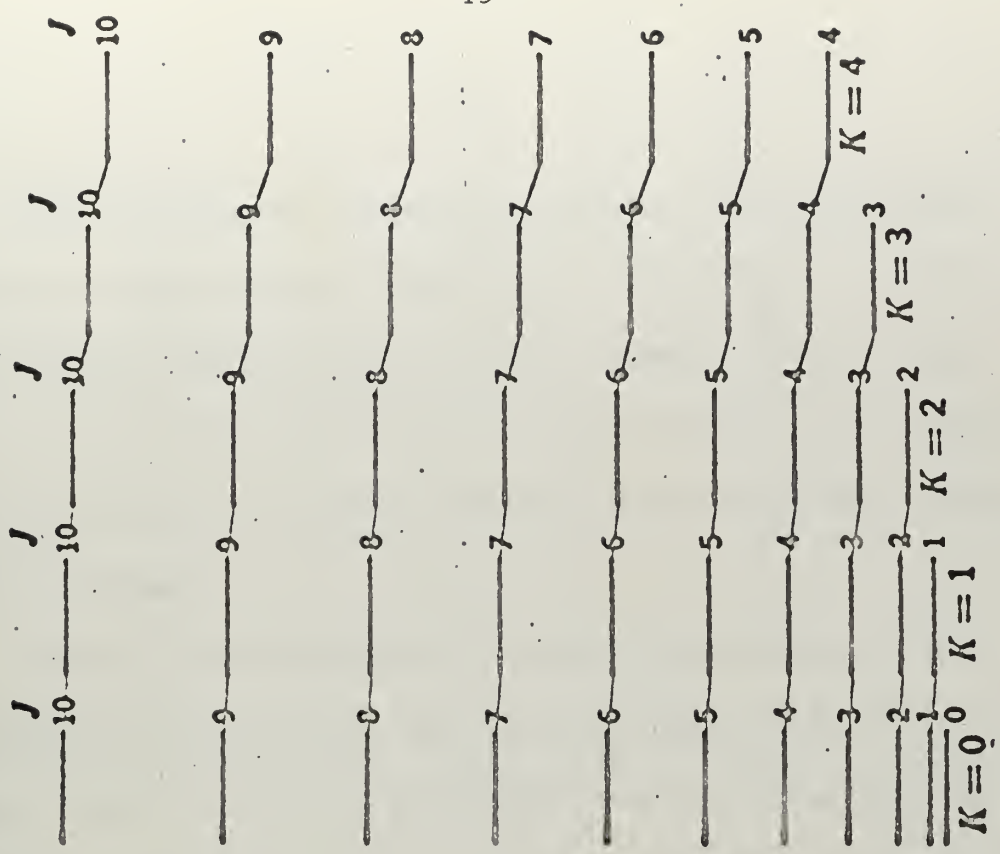
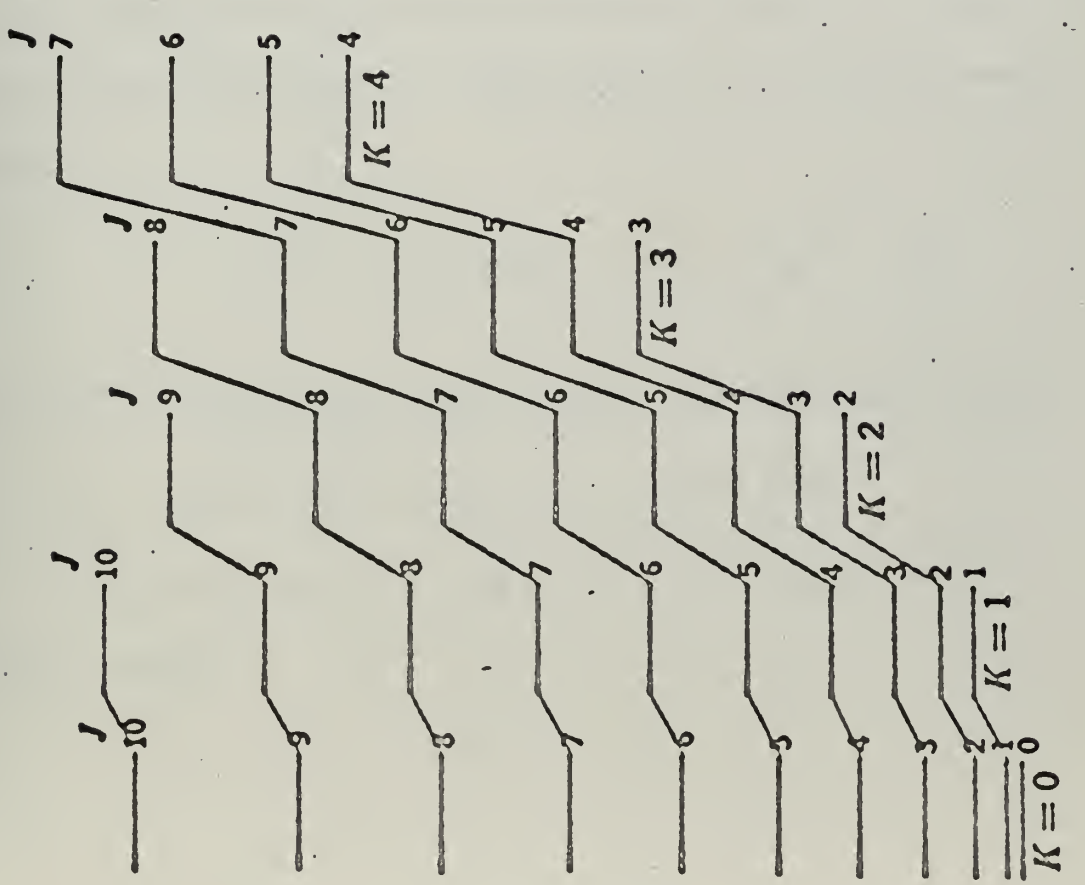


Figure 3. The rotational energy-level patterns for (a) prolate and (b) oblate symmetric-top molecules (From Barrow, p. 107)

Figure 4 illustrates the above discussion on parallel bands and shows its characteristic band contour. Note that the overall or total parallel band consists of various subbands corresponding to the various values of K that occur at the temperature of observation and will appear to consist of one P, one R and a single, strong, line-like Q branch.

Because of the interaction of vibration and rotation and the non-rigidity of the molecule, the rotational constants A_o and B_o characteristic of the ground vibrational state will not be identical to those for the excited vibrational states A' and B' . Thus the subbands do not coincide exactly and the lines of the P and R branch in each subband will not be exactly equidistant but will converge. Perhaps this concept would be made clearer by use of the following equation

$$V_o^{\text{sub}} = V_o + [(A' - A_o) - (B' - B_o)] K^2 \quad (6)$$

where V_o^{sub} is the center of each subband corresponding to a given value of K .

V_o is the center of the overall parallel band

Clearly then, if $A' = A_o$ and $B' = B_o$, the subbands would coincide exactly.

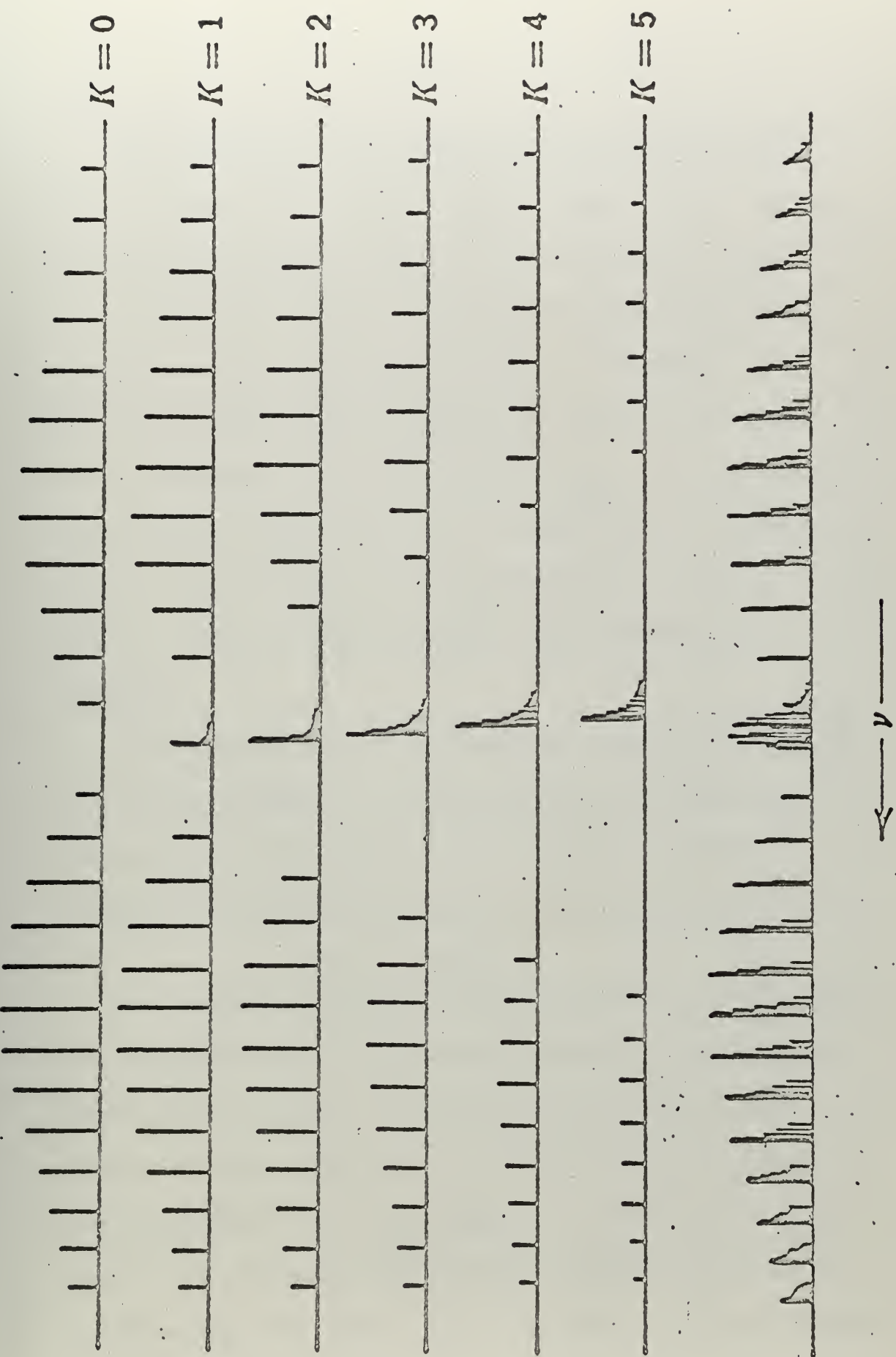


Figure 4. The components of a parallel band showing the contributions from each of the K levels of the $v=0$ state (From Barrow, p. 152).

Also of interest are the relative intensities of the P and R branches versus the Q branch of a parallel band. These relative intensities are a function of I_A/I_B . Thus, if $I_A \ll I_B$, (which indicates only a few K values are of importance) the Q branch is relatively less intense compared to the P and R branches. For example, in a linear molecule such as CO₂ where $I_A = 0$, there isn't any Q branch. In the case of H₂CO, $2 I_A/I_B + I_C = 0.1298$ and for D₂CO, $2 I_A/I_B + I_C = 0.2057$. In other words, a slightly stronger Q branch relative to the P and R branches should be apparent in D₂CO compared to H₂CO. This is confirmed by experiment.

Perpendicular bands of symmetric-top molecules correspond to an oscillating dipole moment perpendicular to the unique axis of the molecule. For such vibrations, the selection rule for rotational transitions accompanying the vibrational transition is

$$\Delta K = \pm 1, \Delta J = 0, \pm 1 \quad (7)$$

The overall perpendicular band observed can, as for a parallel band, be understood as a summation of subbands. Each subband consists of all the $\Delta J = 0, \pm 1$ transitions that occur for a given change in K. Thus, for each $K \rightarrow K + 1$, P, Q, and R subbands result from the $\Delta J = 0, \pm 1$ transitions. For each initial K value, except K = 0, one gets two subbands corresponding to the sets of transitions that occur within $\Delta K = +1$ and $\Delta K = -1$. If the vibration-

rotation interaction is very small (the usual case), the rotational constants can be treated as independent of the vibrational state, and then the different Q branches form a series of equidistant lines with a spacing of $2(A-B)$ (or $2[A-B+C/2]$) for slightly asymmetric molecules such as H_2CO and D_2CO). The spacing can be seen from the energy level expression (4) and the equation for V_o^{sub}

$$V_o^{\text{sub}}(K) = V_o + (A-B) \pm 2(A-B)K \quad (8)$$

where V_o is the band center of the perpendicular band. The intensity of the Q branches with respect to the P and R branches is always large, with the result that the overall band has very strong Q branches with an unresolved background of the P and R branches. For H_2CO and D_2CO where $A \gg B$, the Q branches are well separated (see equation (8)).

If the interaction between vibration and rotation is taken into account, two effects result. First, the rotational constants A and B (and C for an asymmetric top molecule) will not be the same in different vibrational states. Secondly, coriolis coupling between a degenerate pair of vibration occurs which increases with increasing rotation about the principal axis. Coriolis coupling can also occur between two vibrations of slightly different frequencies.

It has been stated that coriolis coupling exists in H₂CO between the fundamental frequencies ν_5 and ν_6 .³ Coriolis coupling is an additional coupling between rotation and vibration and is due to a coriolis force on the rotating nucleii. This force is given in classical mechanics by:

$$F_{\text{coriolis}} = 2 m v_a w \sin d \quad (9)$$

where m is the mass of the particle

v_a its apparent velocity with respect to the moving coordinate system

w is the angular velocity of the coordinate system with respect to a fixed coordinate system

d is the angle between the axis of rotation and the direction of v_a .

The coriolis force occurs only for a moving particle ($v_a \neq 0$)

and is directed at right angles to the direction of motion and at right angles to the axis of rotation.

As a simple example of coriolis interaction, see Figure 5.

It is seen from this figure that during the vibration ν_3 coriolis forces tend to excite the perpendicular vibration ν_2 . If the frequencies ν_2 and ν_3 were nearly the same, a strong excitation of one of the two vibrations would take place if the other were first

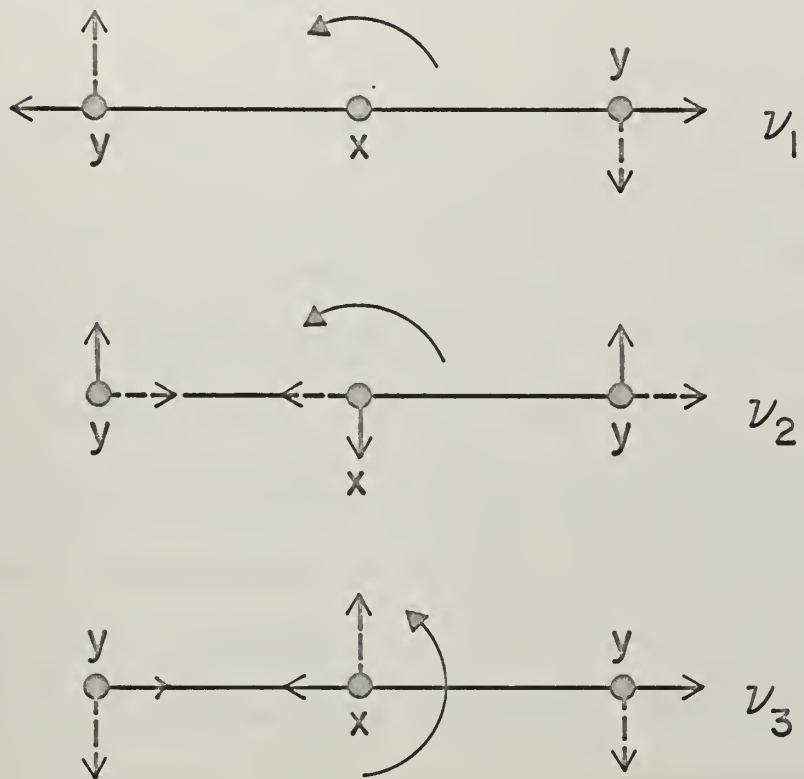


Figure 5. Coriolis forces in linear XY_2 . The curved arrow indicates the direction of rotation. The dashed arrows are the Coriolis forces. (From Herzberg, p. 374).

excited, in consequence of this coriolis coupling. In the case of ν_5 and ν_6 of H_2CO and D_2CO , the difference in frequencies for H_2CO gas is 83.9 cm^{-1} and for D_2CO gas 49.8 cm^{-1} . These frequencies are close enough to have coriolis coupling as proposed by reference 3.

When a fundamental vibration (ν_i) has nearly the same energy as a doubly excited state ($2\nu_k$) or a combination of fundamentals ($\nu_k + \nu_e$), both of which are of the same symmetry species, then an interaction of these eigenfunctions can occur. This perturbation is called Fermi resonance. Simply stated, Fermi resonance can be compared to the classical analog of two coupled pendulums. If one pendulum is set in motion, the resulting vibrations cause a resonance to occur in the second pendulum. In the infrared spectrum, Fermi resonance is recognized by two phenomenon. First, the normally more intense fundamental frequency ν_i will become less intense and the overtone or combination frequency will become more intense. This is called intensity borrowing.

The second effect is that the two vibrational levels having nearly the same energy "repel" each other. One of the levels is shifted up and the other down so that the separation of the two levels is much greater than expected.

Fermi resonance occurs in H_2CO between ν_4 and $\nu_2 + \nu_5^3$.

For D_2CO gas it is possible that Fermi resonance occurs between ν_1 and $2\nu_5$ since both are of the same symmetry species. Twice the frequency of ν_5 is 1975 cm^{-1} but $2\nu_5$ is observed at 1918 cm^{-1} . This will be more thoroughly explained in the discussion on D_2CO gas.

Asymmetric top molecules ($I_A \neq I_B \neq I_C$) have three distinct band types. These are labelled A, B and C depending on whether the dipole moment change occurs along the axis of least, intermediate, or greatest moment of inertia. If the three moments of inertia are considerably different then the resulting bands are indeed extremely complex, and the very simple water molecule is one of the very few cases for which a complete analysis has been achieved. It is only in the limiting case where the molecule approximates a symmetric top that any regularity of fine structures can be expected. In these cases (as in H_2CO and D_2CO) the band structures are determined according to the ratio;

$$p = \frac{I_A}{I_B} \quad (10)$$

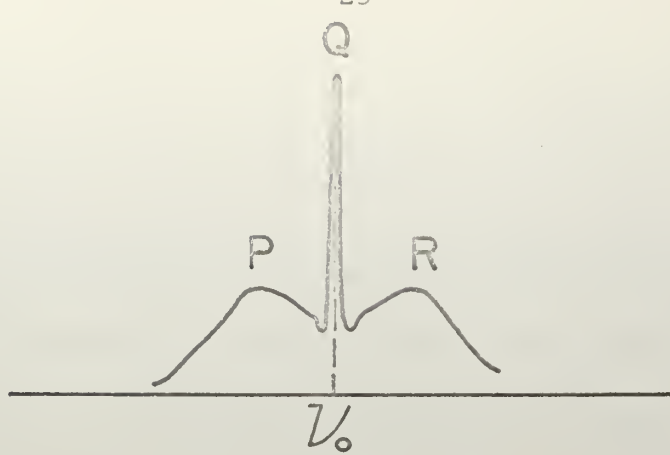
Planar molecules obey the condition

$$I_A + I_B = I_C \quad (11)$$

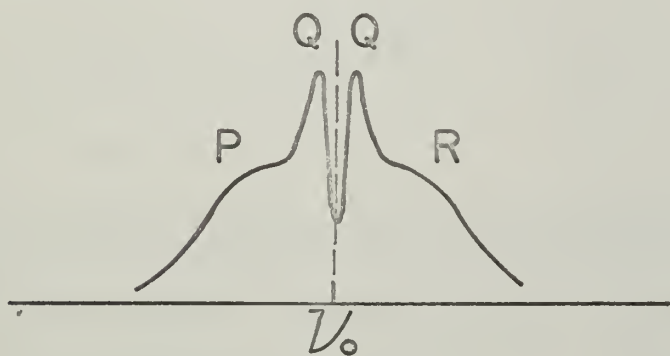
It has been shown that H_2CO is a planar molecule.¹ For these planar molecules, if $p = 1$, then $I_A = I_B < I_C$, which is the condition for an oblate symmetric top; for $p = 0$, $I_A = 0$ and hence $I_B = I_C$, so that this represents a linear molecule. Further, when p is very small (≈ 0.1), $I_B \approx I_C$ and then $I_A < I_B \approx I_C$ which approximates a prolate symmetric top. As has been stated previously, both H_2CO and D_2CO are approximately prolate symmetric tops.

Accordingly, the band contours for dipole transitions along the A, B and C axis resemble the parallel or perpendicular type bands of a symmetric top molecule. In the case of D_2CO and H_2CO , A, B and C type bands resemble parallel and perpendicular bands respectively of a symmetric top. "A" type bands with selection rules $\Delta J=0, \pm 1$, $\Delta K=0$ resemble the parallel band of a symmetric top molecule almost exactly. The type -B and type -C bands, with selection rules $\Delta J = 0, \pm 1$; $\Delta K = \pm 1$, resemble the perpendicular bands of a symmetric top, (ie) a series of Q branches with a separation of $2(A-B+C/2)$. The C-type band is different from the B-type band at the center of the band in that there is a very strong Q branch. The B-type does not have a Q branch at the center of the band. Figure 6 illustrates the above discussion.

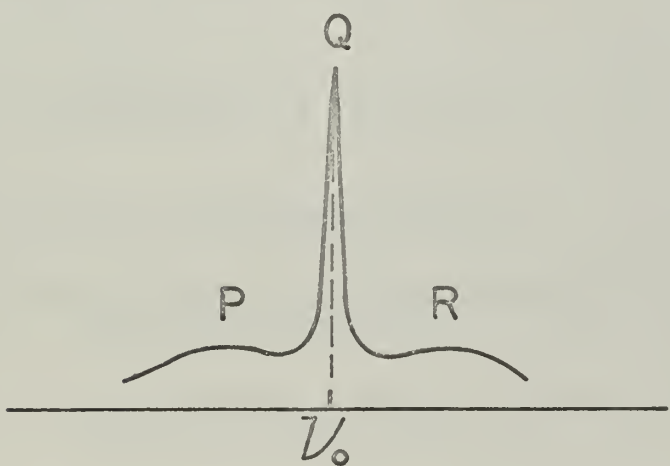
Since the spacing of the Q branches of a B or C type band is



Type - A band ν_1 , ν_2 and ν_3 .



Type - B band ν_4 and ν_5 .



Type - C band ν_6 .

Figure 5. Typical A, B, and C type band contours for D_2CO and H_2CO .
 (From M. Davies, Infrared Spectroscopy and Molecular Structure, Elsevier Pub. Co., 1963 p. 157).

$2(A-B+C/2)$, the rotational constants for H_2CO and D_2CO can be calculated. Note that the spacing of the rotational lines in an A type band is $B + C$ and therefore the value of A can be determined. Knowing the value of A and utilizing equation (11), the following relations can be derived.

$$B = - (A - \tilde{B}) + \sqrt{A^2 + \tilde{B}^2} \quad (12)$$

$$C = (A + \tilde{B}) - \sqrt{A^2 + \tilde{B}^2} \quad (13)$$

where $\tilde{B} = \frac{1}{2} (B + C)$

It is interesting to note that the selection rules for an A type band (parallel) give the allowed transition frequencies for the $v = 0$ to $v = 1$ transition as

$$R(J) = V_o + 2B' + (3B' - B_o) J + (B' - B_o) J^2 \quad (14)$$

$$P(J) = V_o - (B' + B_o) J + (B' - B_o) J^2 \quad (15)$$

where V_o is the fundamental frequency

B' is the rotational constant parallel to the B axis of the excited state

B_o is the rotational constant parallel to the B axis of the ground state.

Using various combinations of $R(J)$ and $P(J)$, the values of B and C for the ground and excited states may be calculated.

Isotopic Substitution

When an atom of a molecule is replaced by its isotope, the vibrational frequencies are very often altered, sometimes appreciably. This comes about not because of any significant change in the potential energy function or geometry of the molecule, since the isotopic substitution leaves the electronic structure essentially unaltered, but because the mass change affects the normal coordinates and the normal modes of vibration. Isotopic substitution is a valuable tool in several ways. In the first place, it may be used to help assign spectral bands to the various normal modes of vibration. Secondly, isotopic frequencies may be needed to provide additional equations for evaluating force constants. Because of the large percentage change in mass involved in the substitution of deuterium for hydrogen, this type of isotopic replacement is particularly effective in studying those normal vibrations which correspond largely to hydrogen atom motions.

The vibrational frequencies of isotopic molecules are related through the well known Teller-Redlich product rule.⁷

⁷ G. Herzberg, Op. Cit., p. 232.

"For two isotopic molecules the product of the ratios of the corresponding zero-order frequencies w^i/w for all vibrations of a given symmetry type (species) is independent of the potential constants and depends only on the masses of the atoms and the geometry of the molecule."

The general formula for any molecule is

$$\frac{w_1^i w_2^i \dots w_\epsilon^i}{w_1 w_2 \dots w_\epsilon} = \sqrt{\left(\frac{m_1}{m_1^i}\right)^\alpha \left(\frac{m_2}{m_2^i}\right)^\beta \dots \left(\frac{M^i}{M}\right)^t \left(\frac{I_x^i}{I_x}\right) \left(\frac{I_y^i}{I_y}\right) \left(\frac{I_z^i}{I_z}\right)}$$

(16)

where all quantities designated by the superscript i refer to the isotopically substituted molecule. The zero-order frequencies w are those vibrational frequencies a molecule would possess were the vibrations strictly harmonic. In (16), $w_1, w_2, \dots w_\epsilon$ are the zero-order frequencies of the various fundamental vibrations belonging to a particular symmetry type; m_1, m_2, \dots are the masses of the representative atoms of the various sets; α, β, \dots are the number of vibrations (inclusive of non-genuine vibrations) each set contributes to the symmetry type considered; M is the

total mass of the molecule; t is the number of translations belonging to the symmetry type considered; I_x , I_y , I_z are the moments of inertia about the x , y and z axis through the center of mass; $\delta_1, \delta_2, \delta_3$ are either 1 or 0 depending on whether or not the rotation about the x , y , or z axis is a non-genuine vibration of the symmetry type considered.

Although (16) should hold rigorously only for the zero-order frequencies w_i , it is at least a good approximation for the observed fundamentals, ν_i . Experience shows that ordinarily the product rule can be expected to hold within 1% to 2%, particularly if the vibrations involve only the more nearly harmonic motions of atoms heavier than hydrogen.

Solid States

Since no well defined rotational energy levels exist in the solid (or liquid) state, the absorption spectrum usually consists of smooth, structureless absorption bands. A number of distinct changes are observed in the crystal lattice compared to the gaseous spectra. The most distinctive feature noted is the increased sharpness of the observed fundamentals. This sharpness, in general, increases with decreasing temperature. Also, slight frequency shifts may take place (from the liquid or gas phase spectra) for the various fundamentals as a result

of molecular interactions caused by the proximity of the molecules to each other in the crystal. In addition, combination bands may appear involving an internal vibration of the molecule with a "lattice mode" of the crystal. Finally, because of the possibility of lower symmetry in the crystal, degeneracies that existed in the free molecule (gaseous state) may be removed, allowing the appearance of more absorption peaks.

Despite these complications, which may or may not be a problem, it is often advantageous to examine the spectra of solid crystalline films since the increased sharpness of the bands might be such that overlapping that often occurs in the gas spectrum is removed or minimized.

The molecules considered in the present study include gaseous and solid formaldehyde and gaseous and solid formaldehyde-
 d_2 .

II. Gaseous Formaldehyde

Introduction

Many studies have been conducted on gaseous formaldehyde.

The most recent infrared study was accomplished by Blau and Nielsen.³ Microwave data^{1, 8, 9, 10} have given accurate figures for the rotational constants of formaldehyde. The following molecular structure information can be derived^{1, 10}

$$r_{CO} = 1.2078 \pm 0.003 \text{ \AA}$$

$$r_{CH} = 1.1161 \pm 0.007 \text{ \AA}$$

$$\angle HCH = 116^\circ 31' \pm 40'$$

$$\angle HCO = 122^\circ 5' \pm 20'$$

The force constants of formaldehyde have previously been

⁸ T. Oka; K. Takagi, and Y. Morino, J. of Mol. Spectroscopy, 14, 27 (1964).

⁹ T. Oka, H. Hirakawa, and K. Shimoda, J. of the Physical Society of Japan, 15, No. 12, 2265 (1960).

¹⁰ K. Takagi and T. Oka, J. of the Physical Society of Japan, 18, No. 8, 1174 (1963).

calculated¹¹ using a computer program to adjust an initial set of force constants in accordance with the requirement that each successive adjustment leads to a smaller sum of squared deviations between calculated and observed eigenvalues.

Formaldehyde has been shown to be a planar molecule^{1, 12} by calculation of the inertia defect. Usually a molecule is said to be planar when the inertia defect $\Delta = I_c - I_b - I_a$ is nearly equal to zero.

Potential energy constants, rotational distortion constants and the thermodynamic properties of formaldehyde have also been calculated.¹³

Since the infrared spectrum of formaldehyde (H_2CO) has been measured fairly recently, no attempt has been made in the present work to restudy this molecule except for one previously unreported band at 3471.8 cm^{-1} . This band was assigned as

¹¹ T. Shimanouchi and I. Suzuki, J. of Chem. Physics, 42, No. 1, 296 (1965).

¹² T. Oka and Y. Morini, J. of Molecular Spectroscopy, 11, 349 (1963).

¹³ M. G. Krishna Pillai and F. F. Cleveland, J. of Molecular Spectroscopy, 6, 465 (1961).

$2\nu_2^a$ and sufficient rotational structure was available to calculate the excited rotational constants, ($B' + C'$), associated with the transition 0-2. This calculation was accomplished with the aid of

$$R(J-1) + P(J) = 4V_o + [(B' + C') - (B_o + C_o)] J^2 \quad (17)$$

By plotting $R(J-1) + P(J)$ vs J^2 and knowing the value of $(B_o + C_o)$ from microwave data,¹ ($B' + C'$) can be found. While equation (17) obviously represents a linear function of $R(J-1) + P(J)$ vs J^2 , experimentally the data rarely give rise to a straight line. Thus, to deduce values for ($B' + C'$), may require an arbitrary treatment of the data.

Experimental

Formaldehyde vapor was prepared by the thermal decomposition of paraformaldehyde using a vacuum apparatus. The vapor was purified by passing it through a series of dry ice-isopropyl alcohol traps. The gas was then collected as a solid in a trap cooled by liquid nitrogen. Purification was necessary due to the presence of impurities such as water vapor and formic acid which are known to catalyze the formation of polymer.¹⁴

¹⁴ J. F. Walker, Formaldehyde, Reinhold Pub. Corp. N. Y. (1953).

Various pressures of gas were introduced into a standard 10 cm gas cell equipped with KBr windows. Absorption spectra were recorded with a Perkin-Elmer 421 dual grating spectrophotometer in the frequency range from $4000 - 550 \text{ cm}^{-1}$.

The maximum time available to record absorption spectra was four hours due to the formation of polyoxymethylene polymer. This polymer was detectable in the absorption spectra from a strong polymer absorption band at 903 cm^{-1} .¹⁵ This is a convenient indication of polymer since H_2CO gas does not have absorption in this region.

The survey spectrum of gaseous H_2CO and the high resolution spectrum of $2\nu_2$ are shown in Figure 7.

Discussion

As previously stated in this introduction, only the unreported band at 3471.8 cm^{-1} has been investigated in the present work. This band is quite strong and exhibits all the characteristics of a type "A" band. The resolving power of the spectrophotometer used was sufficient to allow calculation of the rotational lines.

The assignment of the 3471.8 cm^{-1} band as $2\nu_2 a_1$ is quite obvious for several reasons. The ν_2 fundamental is the most intense

¹⁵ H. Todokoro, et al, The J. of Chem. Phys., 38, No. 3 703 (1963).

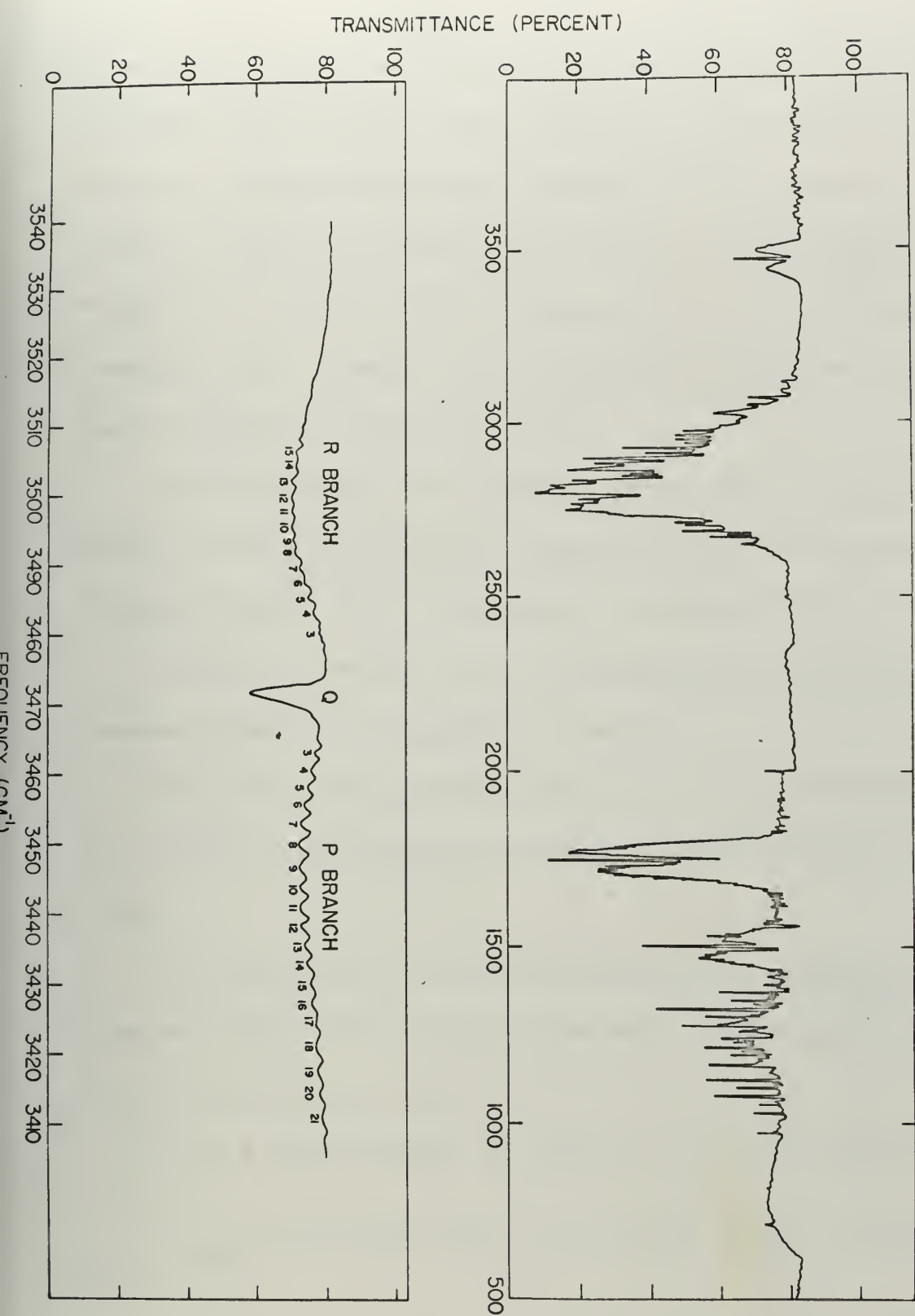


Figure 7. Survey spectrum of gaseous H_2CO (upper frame) and High resolution spectrum of $2\nu_2$ (lower frame).

of all the absorption bands in gaseous formaldehyde. Therefore, one would expect that the first overtone of ν_2 would also be quite intense. Doubling the absorption frequency of ν_2 as given by Nielsen³ would give a value for $2\nu_2$ of 3492.0 cm^{-1} . The actual value of $2\nu_2$ is 3471.8 cm^{-1} , a difference of 20.2 cm^{-1} . No other combinations or overtones of the fundamental frequencies of H_2CO gas are expected near this frequency.

Other evidence of this assignment being correct is the spectral data for solid H_2CO . Only the assignment of $2\nu_2$ for the absorption frequency of 3402.7 cm^{-1} in the solid is possible.^{16, 17}

Further evidence is found in formaldehyde - d₂. where $2\nu_2$ is intense and only this assignment is possible.

Table III gives the frequencies of the P, Q and R branches of $2\nu_2$. Figure 8 represents the application of equation(17) to these data.

It is assumed in this analysis (and all future applications of equation (17)) that for all but the lowest values of the quantum number

¹⁶ K. B. Harvey and J. F. Ogilvie, Can. J. Chem. 40, 85 (1962).

¹⁷ W. G. Schneider and H. J. Bernstein, Trans. Faraday Soc., 52, 13 (1956).

Table III. Infrared rotational frequencies (cm^{-1}) of the P, Q,
and R branches of $2\nu_2 \text{a}_1$. (HCHO gas)

R-Branch ($\Delta J=+1$)	Q-Branch ($\Delta J=0$)	P-Branch ($\Delta J=-1$)
R(15) 3506.8	3471.8	P 21 3413.4
R(14) 3505.1		P 20 3416.8
R 13 3503.1		P 19 3419.9
R 12 3500.9		P(18) 3423.3
R 11 3498.9		P 17 3426.5
R 10 3497.0		P 16 3429.4
R 9 3494.9		P 15 3432.2
R 8 3492.7		P 14 3434.7
R 7 3491.0		P 13 3437.3
R 6 3488.4		P 12 3440.0
R 5 3486.4		P 11 3442.8
R 4 3484.2		P 10 3445.9
R 3 3481.6		P 9 3448.8
R 2 3478.9		P 8 3452.0
R(1) 3476.3		P 7 3454.9
R(0) 3473.3		P 6 3457.3
		P 5 3459.8
		P 4 3462.2
		P 3 3464.4
		P (2) 3466.9
		P (1) 3468.7

() refers to unresolved rotational structure

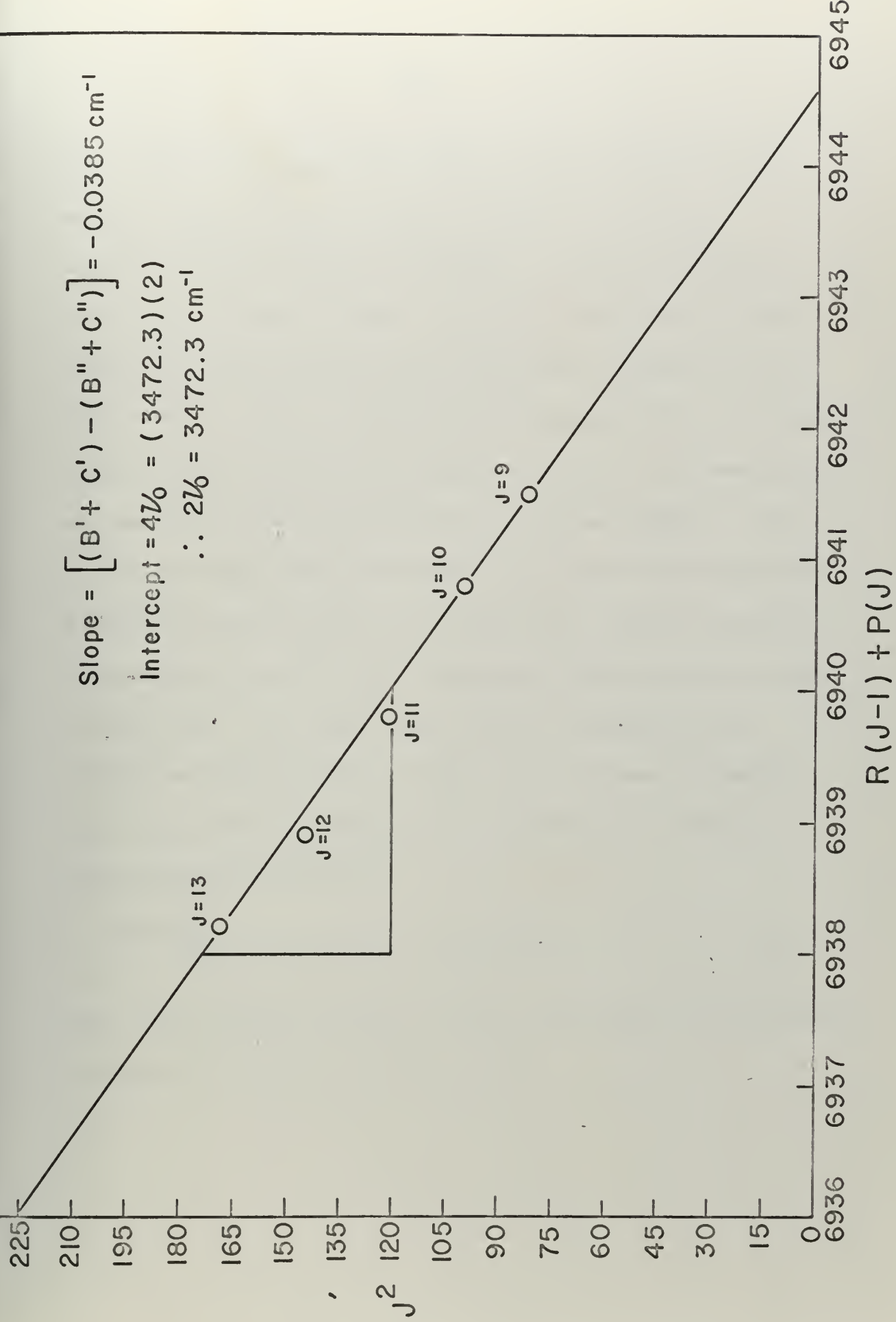


Figure 8.

K(i.e., $K < 3$) the splitting due to the asymmetry of the molecule might be neglected and the molecule treated as a symmetric rotator as proposed by Blau and Nielsen.³ The strong central series of the P and R branches correspond to effective symmetric rotator transitions between levels with K values greater than, say, $K = 3$ or $K = 4$. Because of this, and the fact that for $2\nu_2$ the strong central series is resolved for values of $J = 9$ to $J = 13$, these values of J are used in plotting equation (17), as shown in Figure 8. Note that the intercept of Figure 8 compares favorably with the spectral frequency of the Q branches. The value of $2\nu_0$ from the intercept of equation (17) is 3472.3 cm^{-1} compared to the spectral frequency of 3471.8 cm^{-1} . The value of $(B^i + C^i)$ was calculated by the method described in the introduction. From microwave spectra,¹ $(B_0 + C_0)$ is equal to 2.42962 cm.^{-1} . Therefore, $(B^i + C^i)$ was calculated to be 2.391 cm.^{-1} .

Equation

$$R(J) - P(J+2) = (B_0 + C_0)(2J + 3) \quad (18)$$

leads to an average value of $(B_0 + C_0)$ of 2.4497 cm.^{-1} . This compares favorably with the above microwave value.

Conclusion

The previously unreported band at 3471.8 cm^{-1} has been assigned as $2\nu_2 a_1$. The value of $(B^i + C^i)$ for the excited state of $2\nu_2$ has been evaluated as 2.391 cm^{-1} while the value of $(B_o + C_o)$ for the ground state is 2.449 cm^{-1} compared to the microwave¹ value for $(B_o + C_o)$ of 2.42962 cm^{-1} .

III. Solid Formaldehyde (HCHO)

Introduction

The purpose of examining the infrared spectrum of solid formaldehyde was three-fold.

First, since the polymer of formaldehyde (CH_2O)_n is much cheaper than the polymer of deuterated formaldehyde (CD_2O)_n, solid formaldehyde was used to establish experimental techniques that could be applied to solid formaldehyde-d₂.

Second, in order to have comparable experimental frequencies for the utilization of the Teller-Redlich product rule in assigning the absorption bands of solid D₂CO, solid H₂CO was studied.

Many bands remained unassigned from earlier studies of solid H₂CO.^{16, 17} These bands were attributed to possible crystal splittings. Using isolation techniques, it was possible to verify many bands as truly factor group crystal splittings. A brief discussion of molecular crystals follows which will be of help in understanding crystal splittings.

The vibrational frequencies of the free molecule depends upon its potential energy function V° and associated force constants. If such molecules are condensed into an infinitely large crystal, then

this crystal has an infinite number of vibrational modes comprising lattice as well as intramolecular vibrations. These crystal normal modes can be thought of as consisting of identical vibrational modes in each unit cell, the constant phase difference between the motions in adjacent cells, however, varying from one crystal mode to another. Only those vibrations of the crystal can be active in the infra-red or Raman spectrum in which the molecular motions in any unit cell are in phase with similar vibrational modes in all other unit cells. The unit cell is the smallest volume of the crystal from which the entire crystal can be generated by translations alone. Modes in which the phase difference between unit cell vibration is other than zero give rise effectively to a vanishing transition moment when summed over the crystal. Therefore, in the discussion of fundamental frequencies, one need be concerned only with the analysis of the vibrational modes of molecules within one unit cell of the crystal.

The potential energy associated with the unit cell can be written, in the harmonic approximation, as

$$V = \sum_j (V_j^\circ + V_j^i) + \sum_j \sum_k V_{jk} + V_L + V_{Lj} \quad (19)$$

where the summations extend over all molecules in the unit cell.

The various terms are:

V_j^0 is the potential energy function of the free j^{th} molecule

V_j^1 is the perturbation to V_j^0 due to the equilibrium field of the crystal at the site of the j^{th} molecule.

V_{jk} encompasses interactions between vibrations in different molecules of the unit cell.

V_L contains terms which involve the relative displacement and rotational orientation of molecules with respect to each other, and thus represents the lattice potential.

V_{Lj} denotes those terms involving interaction between lattice coordinates and the internal coordinates of the j^{th} molecule.

The term V_j^1 represents what is usually called site group splitting and is responsible for the shifts in frequency when one compares the spectrum of a gas to its solid. It also is responsible for removing degeneracies due to a lowering of symmetry. The term we are concerned with is the V_{jk} term. This term implies a coupling of vibrations in different molecules of the unit cell. If the unit cell contains N molecules, then a molecular mode of a single molecule will give rise to N crystal modes. The magnitude of this factor group or correlation field splitting is a function of the magnitude of V_{jk} .

By using an experimental technique in which the molecule under examination is in dilute solid solution with an isotopic species, the coupling of the motions of neighboring molecules is removed, thus eliminating the interaction which gives rise to factor group splittings.

This technique was used for HCHO as the molecule under examination and DCDO as the solvent. Molar ratios of 15% and 1% were examined.

Experimental

The polycrystalline solid was obtained by expanding various pressures of HCHO gas into a five liter bulb and then slowly depositing the gas on the AgCl window of a standard cold cell cooled with liquid nitrogen. The rate of deposition greatly affected the absorption spectrum; the sharpest absorption peaks being obtained when the rate of deposition was slow (about 15 minutes). The outside windows of the cold cell were KBr. The advantage of using AgCl for the inside window of the cold cell was because AgCl does not crack at low temperature as does KBr.

The rate of formation of polyoxymethylene polymer was much slower at low temperature and therefore the difficulty involved with gaseous HCHO was avoided.

Dilute HCHO solutions were prepared in the following manner.

Formaldehyde-d₂ gas was produced first and condensed into a 5 liter bulb; then HCHO gas was added. After several mixings of the two gases, the mixture was deposited on the AgCl window as previously described. For the 15% molar solution, 7.5 cm pressure of HCHO and 42.5 cm of DCDO were used; for the 1% solution, 1.0 cm and 99.0 cm were used.

The experimental spectra are shown in Figures 9 and 10 and the frequencies listed in Table IV.

Discussion

The band at 1674.6 cm⁻¹ is probably HC¹³HO since the intensity of this band is about 1% of ν₂. This follows from the fact that C¹³ has a natural abundance of 1.1%. An approximate value of the frequency of the CO stretching mode ν₂ for the C¹³ molecule may be calculated using the expression for the diatomic case

$$\nu^i = \nu \left(\frac{\mu}{\mu_i} \right)^{\frac{1}{2}} \quad (20)$$

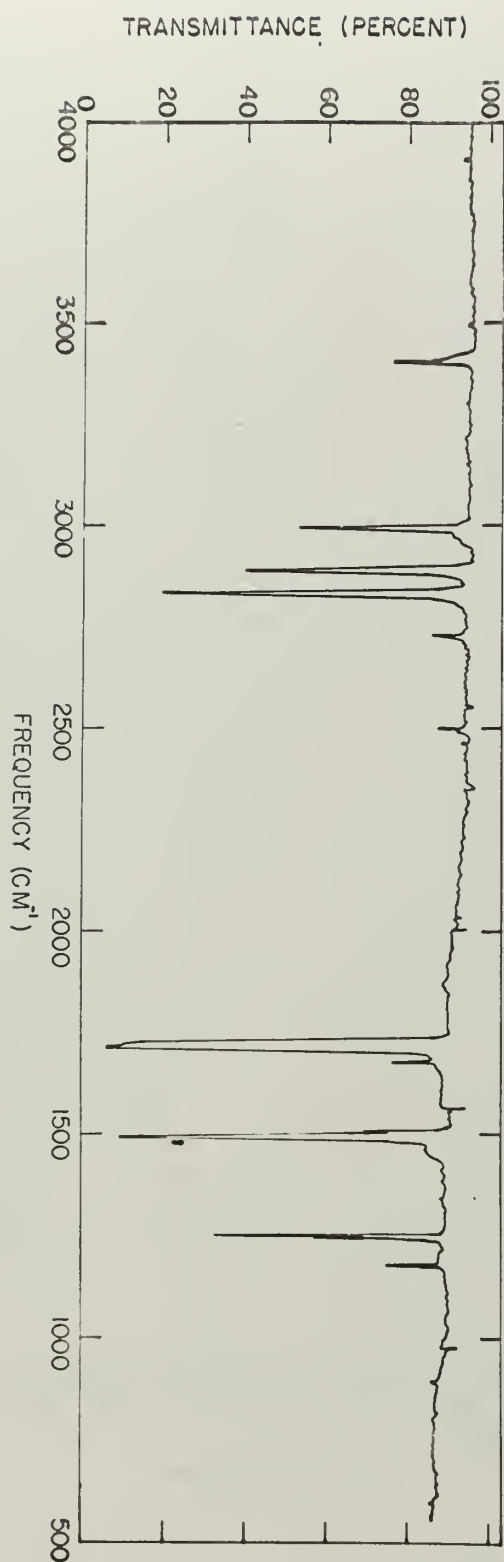


Figure 9. Infrared spectrum of polycrystalline film of HCHO at -190°C .

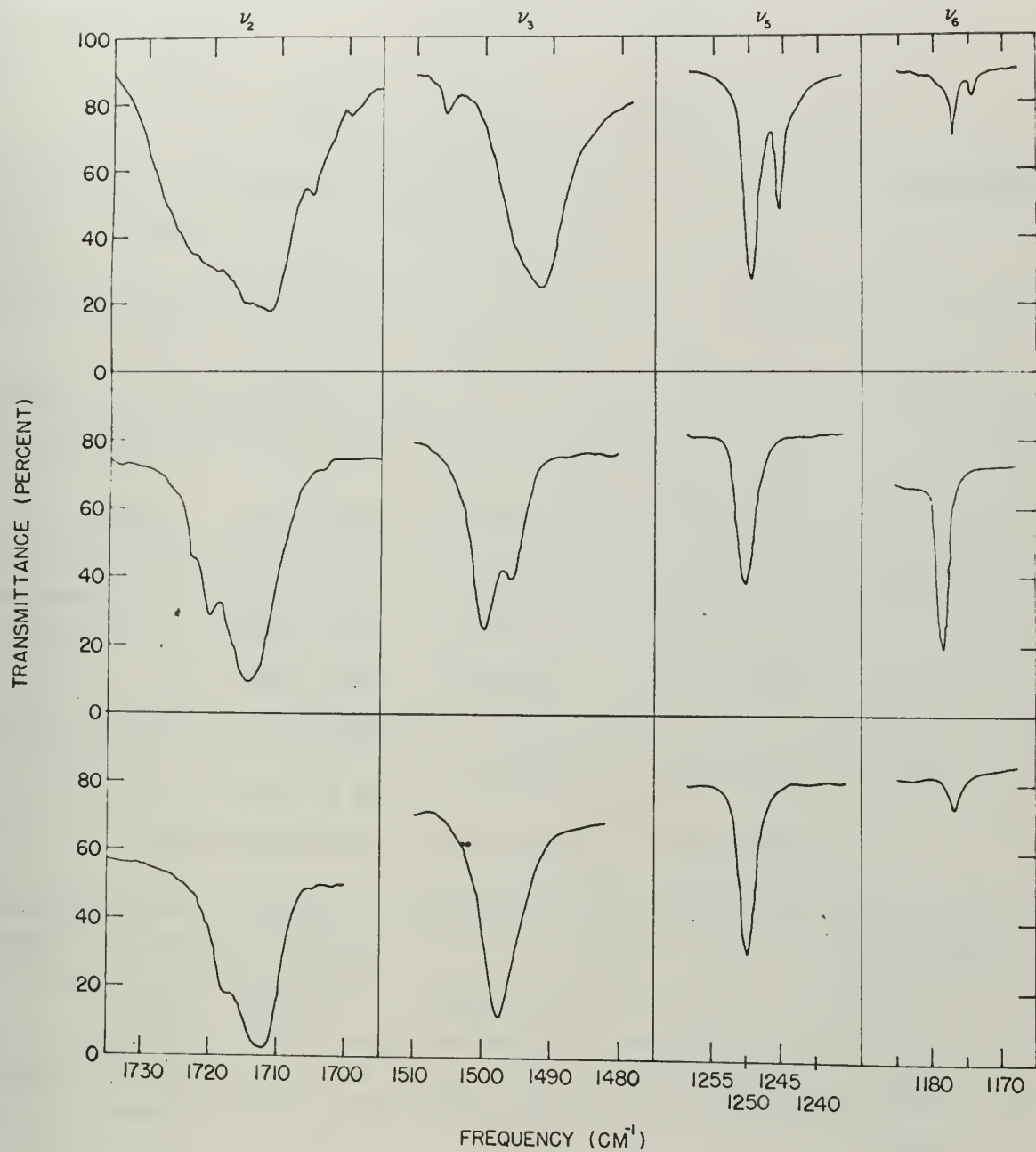


Figure 10. Infrared spectrum of polycrystalline films of pure HCHO at -190°C (upper frame), 15% HCHO in DCDO (middle frame), and 1% HCHO in DCDO (lower frame).

Table IV. A comparison of the vibrational frequencies of polycrystalline and Gaseous HCHO.

Previous Crystal Studies

Gas ³	Schneider ¹⁷ Harvey ¹⁶				15 % HCHO in DCDO	1 % HCHO in DCDO
	and	and	Bernstein	Ogilvie		
			Present			
Work (-190°C)						
					Frequency (cm ⁻¹)	Assignments
1163.5	-----	1174 m	1173.7 m			
	1177 m	1177 s	1176.6 m	1178.0 m	1176.6 m	$\nu_6 b_2$
1247.4	-----	1246 s	1245.5 s			
	1247 m	1250 vs	1249.2 s	1250.0 s	1250.0 s	$\nu_5 b_1$
1500.6	1491 s	1495 vs	1491.6 vs	1495.6 m		
	-----	1506	1505.3 m	1499.2 vs	1497.5 vs	$\nu_3 a_1$
	-----	-----	1674.6 m	-----	-----	$\nu_2 (C^{13})$
	-----	-----	1699.3 sh	-----	-----	
	-----	-----	1705.8 sh	1704.9 sh	1705.7 sh	
1746.0	1712 s	1711 vs	1711.0 vs	1713.9 vs	1712.0 vs	$\nu_2 a_1$
	-----	-----	1713.8 sh			
	-----	1720 sh	1720.7 sh	1719.6 sh	1717.0 sh	
	-----	-----	-----	1722.2 sh	1720.8 sh	
	-----	2729 w	2727 m	2725.6 m		$(\nu_3 + \nu_5) b_1$
2766.4		2834 s	2829 vs	2831.8 vs		$\nu_1 a_1$
2843.4	2890 s	2885 s	2887.1 s			$\nu_4 b_1$
	-----	2960 m	-----	-----		$2\nu_3 a_1$
3003.3	2997 s	2991 vs	2991.6 s			$(\nu_2 + \nu_5) b_1$
3471.8*	3414 w	3402 w	3402.7 m			$2\nu_2 a_1$

w - weak band
sh - shoulder

s - strong band m - medium band vs - very strong
* - Reported by this work.

where ν^i is the absorption frequency of C¹³, ν is the corresponding frequency of C, and μ is the reduced mass of the C-O skeleton.

In this approximation, equation (20) may be written as

$$\nu^i = \nu \left[\frac{(m_C)(m_{C^{13}} + m_O)}{(m_{C^{13}})(m_C + m_O)} \right]^{\frac{1}{2}}$$

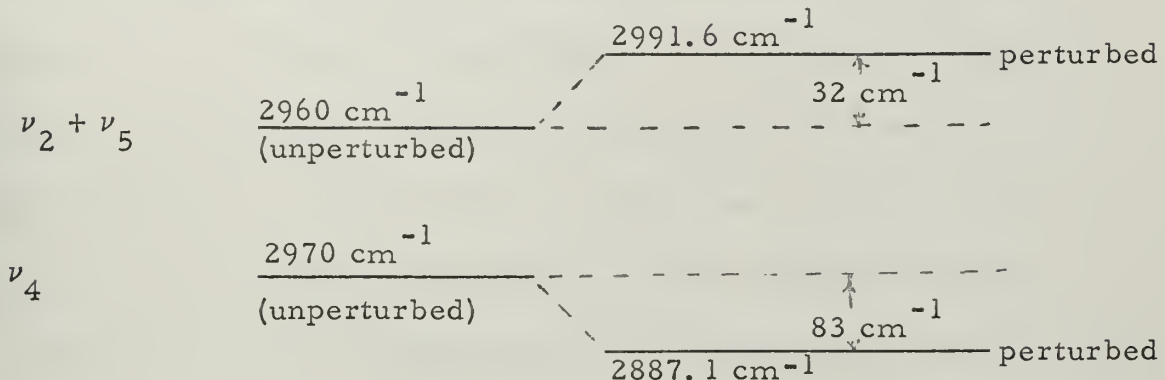
The calculated value of ν^i is 1672.8 cm⁻¹ compared to the observed frequency of 1674.6 cm⁻¹ for ν_2 (C¹³).

As reported by Blau and Nielsen for the gas,³ there is probably Fermi resonance between ν_4 and $\nu_2 + \nu_5$ in the solid as well. The intensity of $\nu_2 + \nu_5$ is nearly as great as that of ν_4 ; an indication of intensity "borrowing". At any rate, the intensity of $\nu_2 + \nu_5$ is much greater than one would expect for a combination band.

For Fermi resonance, one would expect that ν_4 would be shifted to a lower frequency while $\nu_2 + \nu_5$ would move to a higher frequency. Adding ν_2 and ν_5 together results in a frequency of 2960.0 cm⁻¹. This may be taken as an approximate value for the unperturbed state of $\nu_2 + \nu_5$ and compared to the spectral value of 2991.6 cm⁻¹. The unperturbed value of ν_4 may be approximated by using the Teller-

Redlich product rule. This calculated value is 2970 cm^{-1} ; compared to the spectral frequency of 2887.1 cm^{-1} .

The diagram below will make the above results clearer.



While both $\nu_2 + \nu_5$ and ν_4 are shifted in the right direction, the magnitude of the shift is not the same. The explanation for this probably lies in the calculated values for the unperturbed frequencies. Strong evidence for Fermi resonances between ν_4 and $\nu_2 + \nu_5$ still exists, however, due to the magnitude of the intensity of $\nu_2 + \nu_5$ and to the direction of the shifts in frequencies.

Factor group crystal splitting was definitely observed in ν_2 , ν_3 , ν_5 and ν_6 of solid HCHO. This was established by diluting the HCHO with DCDO and, in effect, isolating the HCHO molecules more and more as the solution becomes more dilute. For ν_2 , ν_5 and ν_6 , where the separation of frequencies due to intermolecular

vibration is small, a single frequency resulted when a 15% molar solution was examined.

However, for ν_3 , where the separation is large (13.7 cm^{-1}), the 15% solution retained the two bands although they were closer together (3.6 cm^{-1}) than for pure HCHO. This is characteristic of factor group splitting. Upon further dilution to 1%, the two bands completely merged forming one single band at 1497.5 cm^{-1} which is about half-way between the two bands of the 15% solution.

Near the strong absorption peak of ν_2 , there are two bands which are close together. There is one band at 1711.0 cm^{-1} , the band maxima, and another band at 1713.8 cm^{-1} . Upon dilution, these bands merge to form a single band at 1712.0 cm^{-1} . The other bands of ν_2 are shoulders and are not completely resolved. The band at 1720.7 cm^{-1} for pure HCHO is a very broad shoulder. It is assumed that this broad shoulder is really made up of two bands as evidenced by the two bands for the 15% and 1% solutions in this region. These are not affected by dilution and therefore are not crystal splittings. The shoulder at 1705.8 cm^{-1} is also not affected by dilution and remains unassigned.

Conclusion

From an analysis of the infrared spectrum of solid HCHO and dilute solutions of HCHO in DCDO, factor group crystal splittings were definitely identified for ν_2 , ν_3 , ν_5 and ν_6 . This is convincing evidence that HCHO has at least two molecules per unit cell.

Fermi resonance is probably perturbing ν_4 and $\nu_2 + \nu_5$ in the solid as well as in the gas.

IV. Gaseous Formaldehyde-d₂

Introduction

Since the infrared spectrum of DCDO gas has not been examined recently,² many new assignments have been made in this study. An example of Fermi resonance is seen between ν_1 and $2\nu_5$. There is also evidence of Coriolis resonance interactions among the ν_3 , ν_5 , and ν_6 vibrations.

The rotational constants for the ground state have been calculated from the infrared data. In addition, with the values obtained from microwave data,^{1, 10} the values of (B' + C') for the first excited state of ν_1 , ν_2 and ν_3 were also calculated. Finally, the value of (A' - $\frac{B'+C'}{2}$) has been calculated for ν_4 and ν_5 .

The molecular structure of DCDO as determined from the analysis of microwave data¹⁰ is

$$r_{CO} = 1.2078 \pm 0.003 \text{ } \overset{\circ}{\text{A}}$$

$$r_{CO} = 1.1117 \pm 0.007 \text{ } \overset{\circ}{\text{A}}$$

$$\angle DCD = 116^\circ 37' \pm 40'$$

The potential energy constants, rotational distortion constants, and thermodynamic properties of DCDO have been previously calculated.¹³

Experimental

Formaldehyde-d₂ vapor was prepared in the same manner as HCHO vapor except, of course, polyoxymethylene-d₂ was used as the starting reagent.

The spectrum (see Figure 11) was determined over the same frequency range with the previously described spectrophotometer. The presence of a polymer deposit on the cell window was again detected from the appearance of certain bands in the spectrum, particularly the intense one at 835 cm.⁻¹

Discussion

From the previously established vibrational assignments in gaseous H₂CO and the use of the Teller-Redlich product rule, it was possible to assign all the fundamental frequencies of DCDO gas (Table V). It should be noted that Ebers and Nielsen² did not apply the Teller-Redlich rule correctly to ν₆. The correct expression is



Figure 11. Infrared spectrum of DCDO gas at room temperature.

Table V. A comparison of the vibrational frequencies of gaseous DCDO at room temperature.

Present Work		Ebers and Nielsen ²
Frequency (cm ⁻¹)	Assignments	Frequency (cm ⁻¹)
937.8 w	$\nu_6^{\text{b}_2}$	938 -
987.6 m	$\nu_5^{\text{b}_1}$	990.2
1101.0 s	$\nu_3^{\text{a}_1}$	1106.0
1700.8 s	$\nu_2^{\text{a}_1}$	1700 -
1855.6 vw	* $2\nu_6^{\text{a}_1}$	-----
1918.2 w	* $2\nu_5^{\text{a}_1}$	-----
2057.1 vs	$\nu_1^{\text{a}_1}$	2056.4
2160.3 s	$\nu_4^{\text{b}_1}$	2160.3
2204.0 vw	$2\nu_3^{\text{a}_1}$	2209 -
3383.9 m	* $2\nu_2^{\text{a}_1}$	-----
3755.6 m	* $(\nu_1 + \nu_2)^{\text{a}_1}$	-----
3858.3 w	* $(\nu_2 + \nu_4)^{\text{b}_1}$	-----

* refers to assignments made by the present authors.

$$\left(\frac{\nu_6}{\nu'_6}\right)^2 = \left(\frac{M_D}{M_H}\right) \left(\frac{M_{H_2CO}}{M_{D_2CO}}\right) \left(\frac{I_b}{I'_b}\right)$$

where I_b is the moment of inertia about the intermediate axis and the primes refer to the deuterated species. Table VI shows a comparison of the observed and calculated frequency ratios for H_2CO and D_2CO .

It has already been mentioned that Fermi resonance occurs between ν_1 and $2\nu_5$. The observed frequency of $2\nu_5$, 1918.2 cm^{-1} is shifted significantly downward from twice the value of ν_5 , 1975.2 cm^{-1} . The justification for the assignment of the 1918.2 cm^{-1} band as $2\nu_5$ is two-fold. First, this is the only possible parallel type (a_1) band which would lie close to the observed value. Second, in the spectrum of solid DCDO, this band is apparently shifted upward to 1975.0 cm^{-1} as a result of the disappearance of the Fermi resonance effect. The approximate unperturbed value of ν_1 can be calculated using the Teller-Redlich product rule. The result is 2001 cm^{-1} .

Note that twice the frequency of ν_5 , which should be approximately the frequency of the unperturbed $2\nu_5$ level is 1975.2 cm^{-1} and is therefore separated by only 25.8 cm^{-1} from the unperturbed ν_1 frequency. Since both ν_1 and $2\nu_5$ should shift the same number

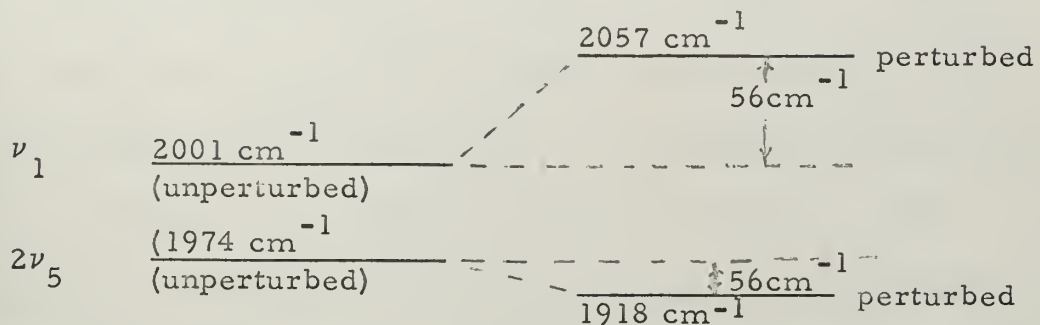
Table VI. Calculated and observed values of the frequency product ratios for DCDO and HCHO gases.

	$\left(\frac{\nu_1^i \nu_2^i \nu_3^i}{\nu_1^i \nu_2^i \nu_3^i} \right)_a^2$	$\left(\frac{\nu_4^i \nu_5^i}{\nu_4^i \nu_5^i} \right)_b^2$	$\left(\frac{\nu_6^i}{\nu_6^i} \right)^2$
Observed	3.5404	2.7647	1.5393
Calculated	3.7418	2.8816	1.5567

a. ν_1^i and ν_3^i are perturbed due to Fermi resonance and Coriolis interaction respectively. This could account for the rather large deviation from calculated values.

b. ν_4^i is perturbed due to Fermi resonance³ and ν_5^i and ν_5^i are perturbed by Coriolis interactions.

of wave numbers upon undergoing Fermi resonance, this can now be checked by the following energy level diagram.



Fermi resonance between ν_1 and $2\nu_5$ apparently does not occur in the solid. This is due to the fact that the levels of ν_1 and $2\nu_5$ are separated by 121 cm^{-1} in the solid. The observed value of $2\nu_5$ in the solid (1975.0 cm^{-1}) is very close to twice the observed value of ν_5 (1976.2 cm^{-1}).

It has been shown¹⁸ that it is possible for ν_3 to undergo a Coriolis interaction with ν_5 or ν_6 , also, ν_5 can interact with ν_6 . It has also been proposed by Blau and Nielsen³ that a significant Coriolis interaction does occur among ν_3 , ν_5 and ν_6 in H_2CO gas.

¹⁸G. Herzberg, Op. cit., p. 466

Although Blau and Nielsen reported a strong convergence of ν_3 toward lower frequencies, a characteristic of Coriolis interaction when the interacting vibrations are very close together¹⁸, none was observed for ν_3 in DCDO gas in the present research. This is surprising in view of the fact that ν_3 in DCDO gas is only 113 cm^{-1} from ν_5 whereas ν_3 in HCHO gas is 253 cm^{-1} from ν_5 . The magnitude of the Coriolis interaction is inversely proportional to the difference in frequency of the two vibrations and therefore one would expect a stronger Coriolis interaction between ν_3 and ν_5 of DCDO gas. According to Herzberg¹⁸, if the two vibrational levels that perturb each other are fairly far apart one obtains simply a change of the rotational constants A, B, and C as compared to the unperturbed values. If the two vibrational levels are very close together one obtains rotational perturbations. Since the value of $(B_o + C_o)$ as calculated from the ν_3 band data (Eq. 18), is 1.58 cm^{-1} compared to the microwave value of 1.95 cm^{-1} it is apparent that ν_3 does have Coriolis interaction with ν_5 , and to some extent, with ν_6 . However, ν_3 is not close enough to ν_5 or ν_6 to have a convergence of rotational lines toward lower frequencies.

Higher resolution spectra of ν_1 , ν_2 , ν_3 , ν_4 , ν_5 and ν_6 are shown in Figures 12 and 13. The observed rotational lines are

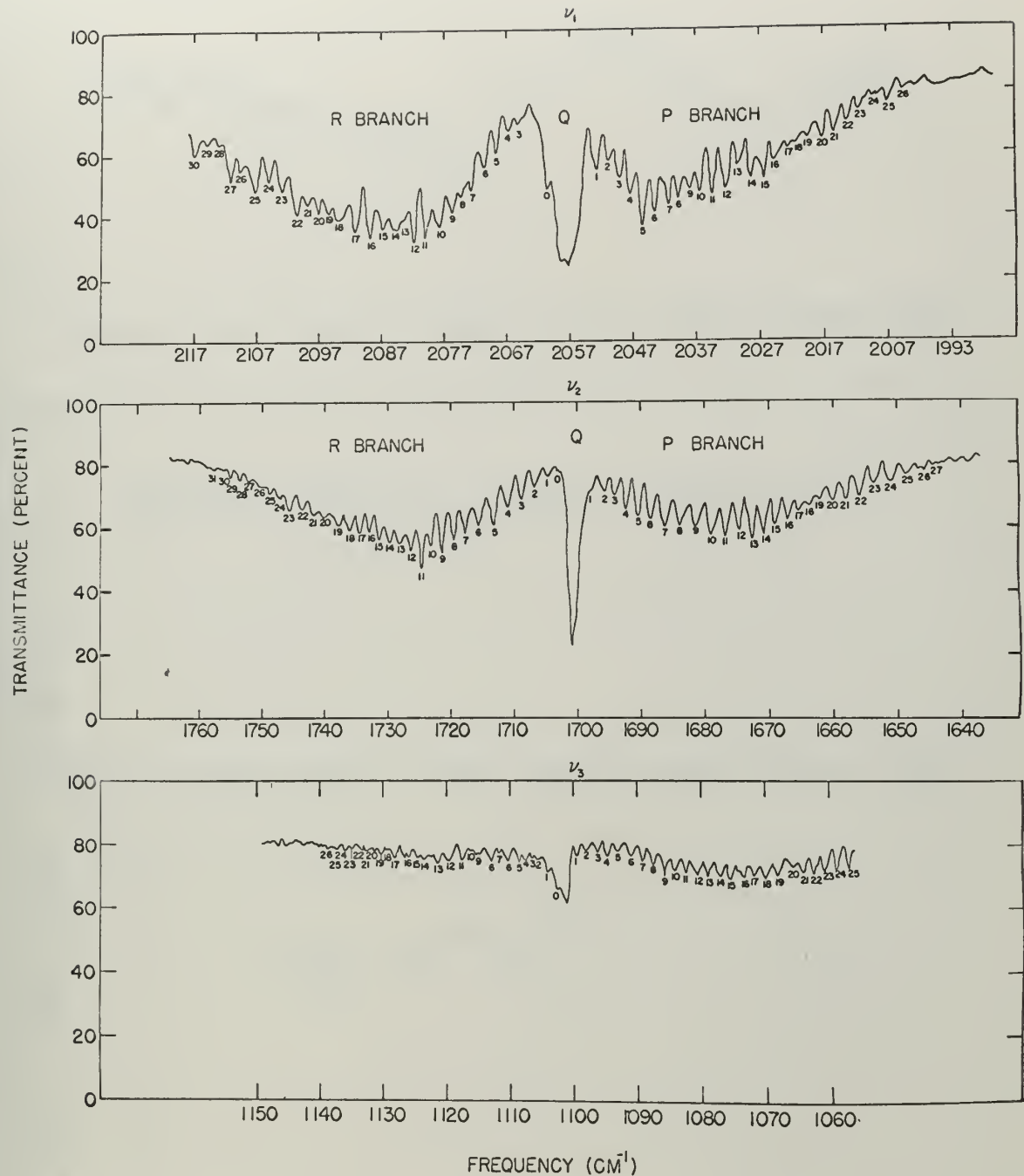


Figure 12. High resolution infrared spectrum of ν_1 , ν_2 and ν_3 .

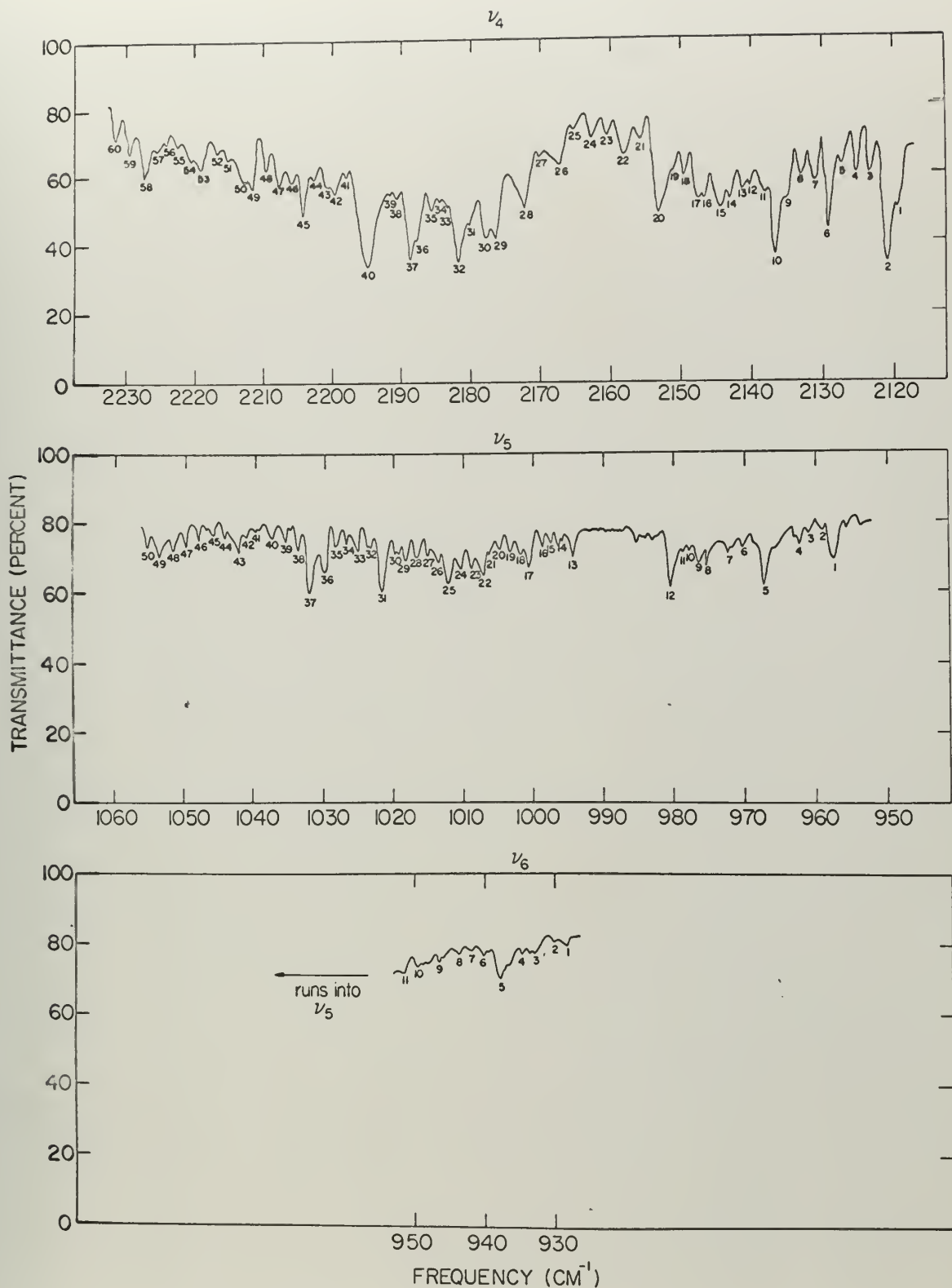


Figure 13. High resolution infrared spectrum of ν_4 , ν_5 and ν_6 .

tabulated in Tables VII, VIII, IX, X, XI, and XII.

Table VII. Infrared rotational frequencies (cm^{-1}) of the P, Q,
and R branches of ν_1 (DCDO gas)

R-Branch ($\Delta J \approx +1$)			Q-Branch ($\Delta J=0$)			P-Branch ($\Delta J = -1$)		
R 30	2116.8	R 7	2072.6	2057.1	P 26	2004.7	P 3	2049.4
R 29	2114.8	R 6	2070.6		P 25	2007.1	P 2	2051.1
R 28	2113.2	R 5	2068.5		P 24	2009.3	P 1	2053.0
R 27	2111.3	R 4	2066.6		P 23	2011.6		
R 26	2109.6	R 3	2065.2		P 22	2013.9		
R 25	2107.2	R 2	-----		P 21	2015.8		
R 24	2105.2	R 1	2062.4		P 20	2017.7		
R 23	2102.9	R 0	2060.5		P 19	2019.7		
R 22	2100.8				P 18	2021.6		
R 21	2098.9				P 17	2022.7		
R 20	2096.9				P 16	2024.8		
R 19	2095.1				P 15	2026.4		
R 18	2093.7				P 14	2028.3		
R 17	2091.3				P 13	2030.2		
R 16	2089.1				P 12	2032.2		
R 15	2086.6				P 11	2034.0		
R 14	2084.9				P 10	2036.1		
R 13	2083.5				P 9	2037.8		
R 12	2081.8				P 8	2039.8		
R 11	2080.0				P 7	2041.4		
R 10	2077.7				P 6	2043.6		
R 9	2075.7				P 5	2045.8		
R 8	2074.3				P 4	2047.6		

Table VIII. Infrared rotational frequencies (cm^{-1}) of the P, Q, and R Branches of ν_2 (DCDO gas).

R-Branch ($\Delta J = +1$)		Q-Branch ($\Delta J = 0$)		P-Branch ($\Delta J = -1$)				
R 31	1759.2	R 8	1719.2	1700.8	P 27	1645.0	P 4	1691.9
R 30	1757.5	R 7	1717.1		P 26	1646.4	P 3	1694.0
R 29	1756.0	R 6	1715.1		P 25	1649.1	P 2	1695.8
R 28	1754.3	R 5	1713.0		P 24	1651.5	P 1	1697.7
R 27	1752.7	R 4	1711.0		P 23	1654.1		
R 26	1750.6	R 3	1709.0		P 22	1656.2		
R 25	1748.9	R 2	1707.3		P 21	1658.2		
R 24	1746.6	R 1	1705.3		P 20	1660.3		
R 23	1745.2	R 0	1703.5		P 19	1662.1		
R 22	1743.2				P 18	1663.7		
R 21	1741.2				P 17	1665.6		
R 20	1739.6				P 16	1667.6		
R 19	1737.5				P 15	1669.4		
R 18	1735.8				P 14	1671.2		
R 17	1734.2				P 13	1673.0		
R 16	1732.8				P 12	1675.3		
R 15	1731.3				P 11	1677.2		
R 14	1730.0				P 10	1679.2		
R 13	1728.7				P 9	1681.5		
R 12	1727.2				P 8	1684.0		
R 11	1725.7				P 7	1686.4		
R 10	1724.2				P 6	1688.3		
R 9	1721.9				P 5	1690.1		

Table IX. Infrared rotational frequencies (cm^{-1}) of the P, Q, and R branches of ν_3 (DCDO gas).

R-Branch ($\Delta J = +1$)	Q-Branch ($\Delta J = 0$)	P-Branch ($\Delta J = 1$)
R 30 1147.3	R 8 1113.1	P 34 1041.3
R 29 1145.6	R 7 1111.8	P 33 1042.5
R 28 1143.1	R 6 1110.5	P 32 1044.2
R 27 1140.8	R 5 1108.8	P 31 1046.0
R 26 1139.0	R 4 1107.4	P 30 1047.9
R 25 1137.5	R 3 1106.5	P 29 1050.2
R 24 1135.8	R 2 1105.3	P 28 1051.9
R 23 1134.9	R 1 1104.2	P 27 1053.7
R 22 1133.5	R 0 1102.4	P 26 1055.4
R 21 1132.9		P 25 1057.1
R 20 1131.6		P 24 1059.0
R 19 1130.6		P 23 1060.8
R 18 1129.3		P 22 1062.8
R 17 1128.3		P 21 1064.3
R 16 1126.7		P 20 1066.0
R 15 1125.0		P 19 1068.2
R 14 1123.8		P 18 1070.1
R 13 1121.6		P 17 1071.7
R 12 1120.0		P 16 1073.5
R 11 1117.7		P 15 1075.4
R(10) 1115.6		P 14 1077.2
R 9 1115.2		P 13 1078.9

() refers to unresolved branches

Table X. Infrared spectral frequencies for the type "B" band,
 ν_4 . (DCDO gas).

Q-branches	Line* No.	Frequency (cm ⁻¹)	Q-branches	Line* No.	Frequency (cm ⁻¹)
P_{Q_5}	1	2119.1	R_{Q_0}	24	2162.7
	2	2120.3		25	2165.1
	3	2122.8		26	2167.2
	4	2124.7		27	2169.9
P_{Q_4}	5	2126.7	R_{Q_1}	28	2172.1
	6	2128.8		29	2176.1
	7	2130.7		30	2177.7
	8	2132.8		31	2180.2
P_{Q_3}	9	2135.0	P_{Q_3}	32	2181.6
	10	2136.6		33	2183.1
	11	2137.9		34	2184.3
	12	2140.0		35	2185.6
P_{Q_2}	13	2141.1	P_{Q_4}	36	2187.5
	14	2142.9		37	2188.4
	15	2144.3		38	2189.1
	16	2146.5		39	2191.0
P_{Q_1}	17	2147.5	P_{Q_5}	40	2194.4
	18	2149.5		41	2197.7
	19	2150.8		42	2199.5
	20	2153.0		43	2200.5
	21	2155.6	P_{Q_6}	44	2202.3
	22	2158.1		45	2204.0
	23	2160.6		46	2205.8

* See Figure 13 for line assignments.

Table X - Continued

Q-branches	Line* No	Frequency (cm ⁻¹)	Q-branches	Line* No	Frequency (cm ⁻¹)
R_{Q_7}	47	2207.5	(R_{Q_9})	54	2220.2
	48	2209.4		55	2222.1
	49	2211.4		56	2223.8
	50	2212.6		57	2225.1
	51	2214.9		58	2227.0
	52	2216.4		59	2229.1
(R_{Q_8})	53	2218.7		60	2231.2

() refers to an uncertain assignment of a Q-branch.

Table XI. Infrared spectral frequencies for the type "B" band,
 ν_5 . (DCDO gas).

Q-branches	Line* Frequency		Q-branches	Line* Frequency	
	No.	(cm)		No.	(cm)
P_{Q_5}	1	956.9		26	1013.4
	2	958.7		27	1015.1
	3	960.5		28	1016.6
P_{Q_4}	4	961.9		29	1018.4
	5	967.3		30	1019.5
	6	970.1	R_{Q_3}	31	1021.5
P_{Q_3}	7	972.2		32	1023.3
	8	975.8		33	1025.2
	9	976.9		34	1026.7
P_{Q_2}	10	978.3		35	1028.4
	11	978.9		36	1029.9
	12	980.5	R_{Q_4}	37	1031.9
R_{Q_0}	13	994.4		38	1033.9
	14	996.2		39	1035.8
	15	997.2		40	1037.6
R_{Q_1}	16	998.6		41	1039.3
	17	1000.6		42	1041.3
	18	1001.7	(R_{Q_5})	43	1042.5
R_{Q_1}	19	1003.3		44	1044.2
	20	1004.9		45	1046.0
	21	1006.1		46	1047.9
R_{Q_2}	22	1007.2		47	1050.2
	23	1008.5		48	1051.9
	24	1010.3	(R_{Q_6})	49	1053.7
R_{Q_2}	15	1011.8		50	1055.4

* See Figure 13 for line assignments.

Table XII. Infrared spectral frequencies for the type "C" band, ν_6 . (DCDO gas).

Line No.*	Frequency(cm^{-1})	Line No.	Frequency (cm^{-1})
1	917.7	7	942.1
2	929.3	8	943.9
3	932.2	9	946.5
4	934.3	10	949.0
5	937.8	11	951.0
6	940.3		

* See figure 13 for line assignments.

Note: Q-branches were not assigned for this band since ν_6 is a weak band and it was not possible to identify these lines.

Using equation (18) where B_o and C_o are the rotational constants for the ground state, an average value of $(B_o + C_o)$ may be calculated for ν_1 , ν_2 and ν_3 . From the type "B" bands, ν_4 and ν_5 , the value of $A_o - (\frac{B_o + C_o}{2})$ may be obtained with the aid of

$$R_{Q_{K-1}} - P_{Q_{K+1}} = 4 (A_o - \frac{B_o + C_o}{2}) K \quad (21)$$

where A_o is the rotational constant for the ground state about the unique axis.

By plotting the relation

$$R(J-1) + P(J) = 2V_o + [(B^1 + C^1) - (B_o + C_o)] J^2 \quad (22)$$

for ν_1 , ν_2 and ν_3 , the values of the first excited state rotational combination constant $(B^1 + C^1)$ may be calculated since $(B_o + C_o)$ is known from microwave data.¹ Note that the intercept, $2\nu_o$, is a good check on the assigned vibrational frequency for the fundamental. In plotting equation (22), the "lines" which correspond to effective symmetric rotator transitions between levels with K values greater than $K = 3$ or $K = 4$ stand out rather sharply. The values of J used were from about $J = 8$ to $J = 16$ since these transitions

correspond to the strong central series of the P and R branches.

The central series is least affected by assymetry and the molecule may be treated as a symmetric rotator. This is the same procedure as used by Blau and Nielsen in their study of formaldehyde vapor.³

For the plot of equation (22) see figures 14 through 16.

With the aid of

$$R_{Q_K} - P_{Q_K} = 4 \left(A^i - \frac{B^i + C^i}{2} \right) K \quad (23)$$

the value of $\left(A^i - \frac{B^i + C^i}{2} \right)$ may be calculated for ν_4 and ν_5 .

In Table XIII, the values of all the rotational constants determined in this study for DCDO gas are compared with previous microwave studies.⁸ Note that previous data for ν_1 and ν_5 are not available.

The rotational constants for ν_6 could not be determined since this is a weak band and the Q branches could not be identified.

Conclusion

Many new assignments have been made for DCDO gas. The rotational combination constants have been calculated for several first excited states and the rotational constants for the ground state have been calculated and compared to microwave data.

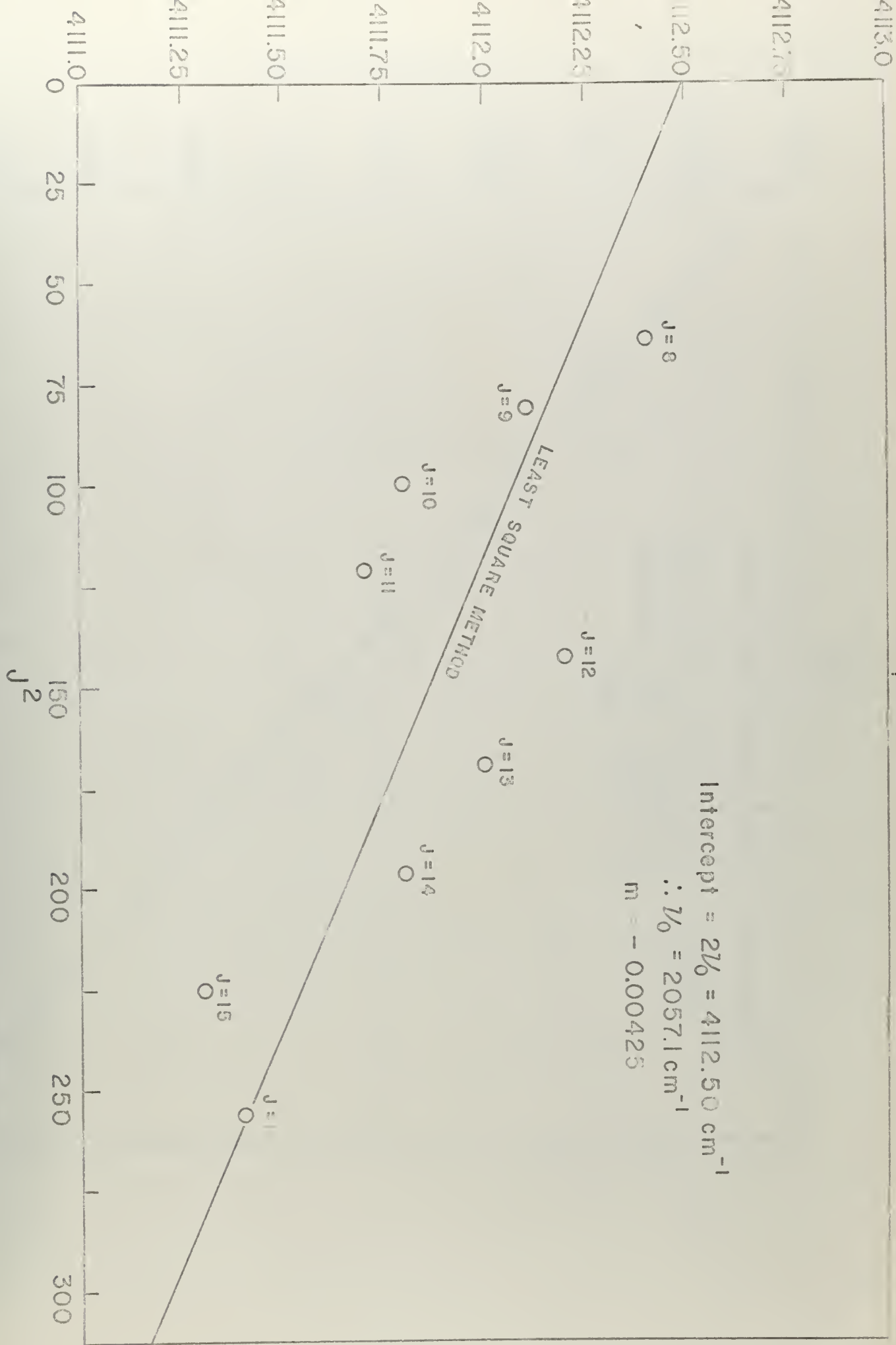


Figure 14.

ν_2

$$R(J-1) + P(J) = 2\nu_0 + [(B' + C') - (B_0 + C_0)] J^2$$

3402

3401

3400

3399

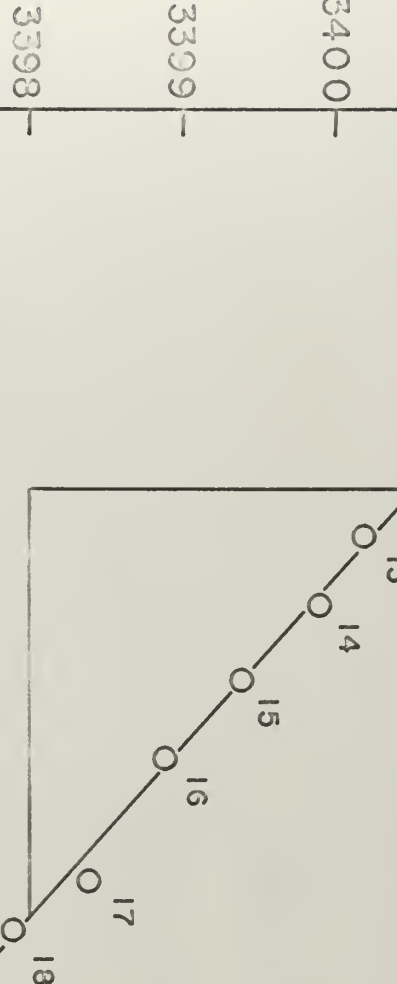
3398

3397

3396

$$\begin{aligned} \text{Slope} &= (B' + C') - (B_0 + C_0) = -0.01500 \\ \text{Intercept} &= 2\nu_0 = 3402.77 \\ \therefore \nu_0 &= 1701.4 \text{ cm}^{-1} \end{aligned}$$

$R(J-1) + P(J)$



v_3

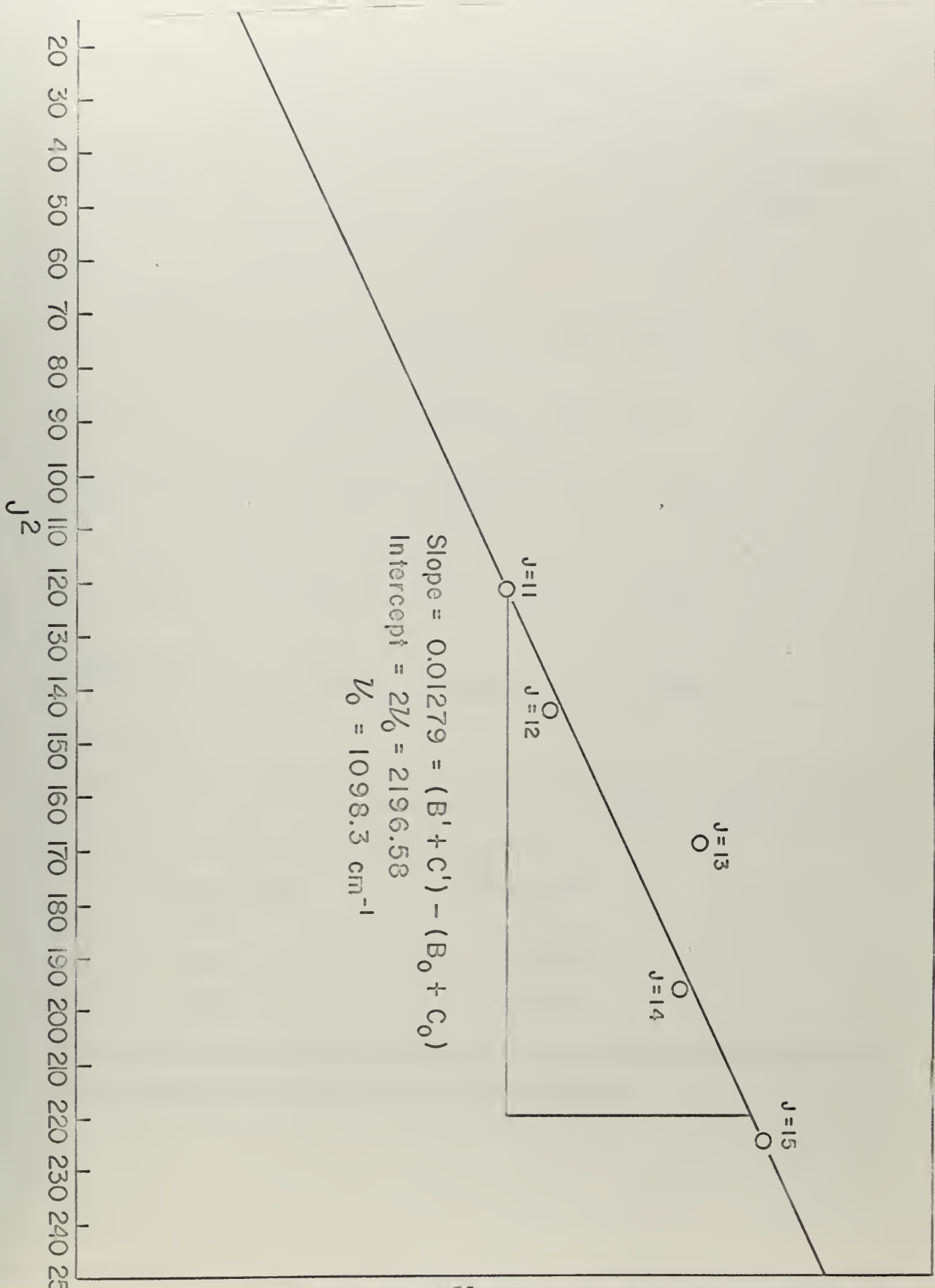


Figure 16

Table XIII. A comparison of Rotational constants (cm^{-1}) for
the ground state and first excited state of Gaseous DCDO.

Rotational Constants	ν_1	ν_2	ν_3	ν_4	ν_5	Microwave Value
$(B_0 + C_0)$	1.99	2.02	1.58	----	----	1.95
$A_0 - \frac{(B_0 + C_0)}{2}$	----	----	----	3.89	4.03	3.75
$(B' + C')$	1.946	1.935	1.963	----	----	
Microwave Values of $(B' + C')$	----	1.93688	1.96637	----	1.94733	
$A' - \frac{(B' + C')}{2}$	----	----	----	3.73	4.22	
Microwave Values of $A' - \frac{(B' + C')}{2}$	----	3.75825	3.77287	----	4.22005	

Using values above, the individual rotational constants from the present work and microwave data may be determined.

	<u>Present Work</u>	<u>Microwave</u>
A_0	4.83	4.72539
B_0	1.03	1.07692
C_0	0.85	0.87354

The ground state and the first excited state are designated respectively by the subscript zero and the prime superscript.

An example of Fermi resonance between ν_1 and $2\nu_5$
has been observed.

There is also evidence of coriolis resonance interaction
among ν_3 , ν_5 and ν_6 .

V. Polycrystalline DCDO

Introduction

The infrared spectrum of solid DCDO has not been previously studied. Using the Teller-Redlich product rule and the spectrum of solid HCHO, all the fundamental frequencies of solid DCDO were assigned. The infrared spectrum of DCDO gas was also helpful as a guide in the assignments.

The infrared spectrum of solid DCDO was in turn of great aid in making the assignments of gaseous DCDO since the solid spectrum, with no rotational structure and sharper bands, is less complicated.

Unlike solid HCHO where factor group crystal splitting was observed for ν_2 , ν_3 , ν_5 and ν_6 , no cases of crystal splitting were observed in solid DCDO. This means that the ν_{jk} term of equation (19) is much smaller for DCDO than for HCHO. In other words, interaction between vibrations in different molecules of the unit cell is small for DCDO as compared to HCHO.

Experimental

Preparation of solid DCDO was accomplished in the same

manner as for solid HCHO except that $(CD_2O)_n$ polymer was used as the starting reagent. The spectrum is shown in Figure 17.

Discussion

The only impurity noted in the infrared spectrum of solid DCDO was a trace of HDCO. Since the infrared spectrum of HDCO had previously been studied,¹⁹ these bands were easily identified.

Listed in Table XIV are the assignments and frequency shifts of polycrystalline DCDO.

The following Teller-Redlich product rule relations were used in assigning the fundamental frequencies of crystalline DCDO:

$$\left(\frac{\nu_1}{\nu'_1} \frac{\nu_2}{\nu'_2} \frac{\nu_3}{\nu'_3} \right)^2 = \left(\frac{m_D}{m_H} \right)^2 \left(\frac{M_{H_2CO}}{M_{D_2CO}} \right)$$

$$\left(\frac{\nu_4}{\nu'_4} \frac{\nu_5}{\nu'_5} \right)^2 = \left(\frac{m_D}{m_H} \right)^2 \left(\frac{M_{H_2CO}}{M_{D_2CO}} \right) \left(\frac{I_c}{I'_c} \right)$$

$$\left(\frac{\nu_6}{\nu'_6} \right)^2 = \left(\frac{m_D}{m_H} \right) \left(\frac{M_{H_2CO}}{M_{D_2CO}} \right) \left(\frac{I_b}{I'_b} \right)$$

¹⁹ D. Davidson, B. P. Stoicheff, and H. J. Bernstein, J. of Chem. Phys., 22, No. 2, 289 (1954).

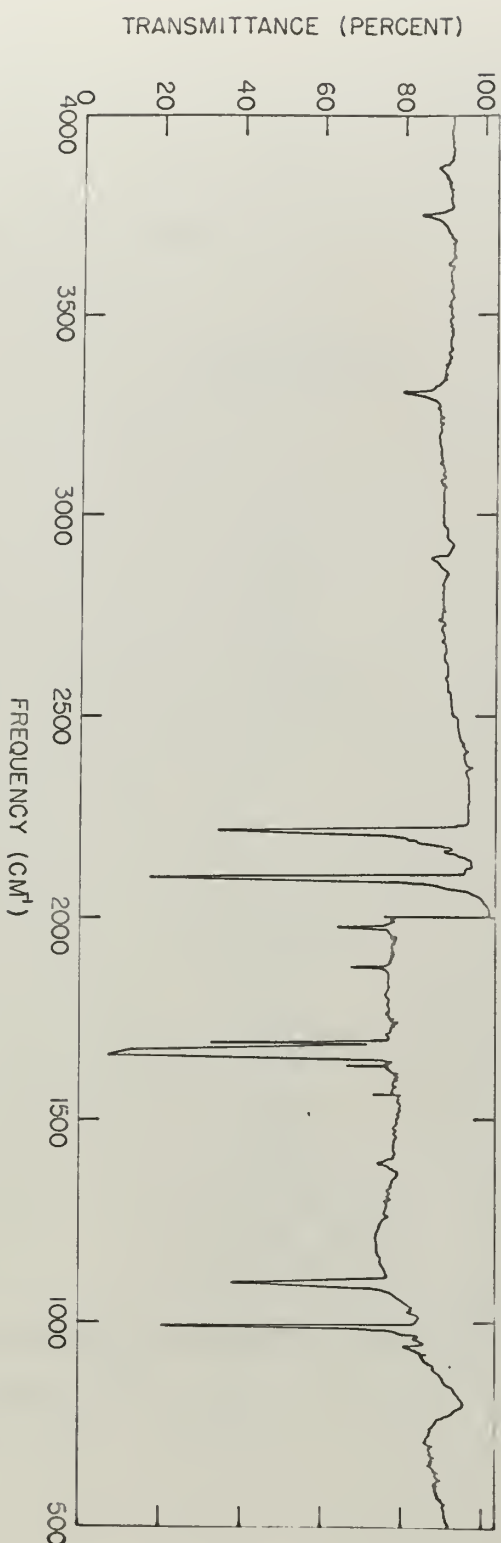


Figure 17. Infrared spectrum of polycrystalline DCDO at -190°C .

Table XIV. Band Centers (cm^{-1}), Frequency Shifts, and
Assignments for the Infrared Spectrum of
Polycrystalline DCDO. ($\sim 190^\circ \text{C}$)

Frequency (cm^{-1})	Assignments	Frequency Shift ¹
941.5 w	$\nu_6^{\text{b}}_2$	- 3.7
988.1 s	$\nu_5^{\text{b}}_1$	- 0.4
1095.6 s	$\nu_3^{\text{a}}_1$	+ 5.4
1633.0 m	$\nu_2^{\text{(C}^{13}\text{)}}$	
1658.6 vs	ν_2	+ 42.2
1667.5	sh	
1874.7 m	$2\nu_6^{\text{a}}_1$	
1975.0 m	$2\nu_5^{\text{a}}_1$	
2095.5 s	$\nu_1^{\text{a}}_1$	- 38.4
2162.5 w	$2\nu_3^{\text{a}}_1$	
2213.7 s	$\nu_4^{\text{b}}_1$	- 53.4
3305.3 m	$2\nu_2^{\text{a}}_1$	
3748.9 m	$(\nu_1 + \nu_2)^{\text{a}}_1$	
3868.8 w	$(\nu_2 + \nu_4)^{\text{b}}_1$	

1. $\nu_{\text{gas}} - \nu_{\text{solid}}$, in cm^{-1} .

where m_D is the mass of deuterium m_H is the mass of hydrogen,

M_{H_2CO} is the molecular weight of formaldehyde and

M_{D_2CO} is the molecular weight of formaldehyde-d₂.

I_c is the largest principal moment of inertia and

I_b is the intermediate moment of inertia.

The primes refer to the corresponding isotopic values. ν_1' , ν_2' , ...

ν_6 are the band centers of polycrystalline formaldehyde and ν_1^t ,

ν_2^t ... ν_6^t are the corresponding values for polycrystalline

formaldehyde-d₂. Table XV lists the calculated and observed values
for these relationships.

Conclusion

Since factor group crystal splitting was not observed for
polycrystalline DCDO, it follows that there is a smaller interaction
between the molecules of the unit cell than for polycrystalline
HCHO.

All the fundamental frequencies were assigned as were several
combination and overtone bands.

Table XV. A comparison of Observed and calculated product rule ratios for polycrystalline DCDO and HCHO.

	$\left(\frac{\nu_1 \nu_2 \nu_3}{\nu'_1 \nu'_2 \nu'_3} \right)^2$	$\left(\frac{\nu_4 \nu_5}{\nu'_4 \nu'_5} \right)_a^2$	$\left(\frac{\nu_6}{\nu'_6} \right)^2$
Observed	3.6014	2.7214	1.5618
Calculated	3.7418	2.8816	1.5567

a ν_4 is in Fermi resonance with $\nu_2 + \nu_5$. The unperturbed value of ν_4 is at a higher frequency, thus bringing the observed value closer to the calculated value.

b The primes refer to the deuterated species.

سیاه کاری
کتابخانه ملی افغانستان

thesH8274
The infrared spectra of formaldehyde and



3 2768 002 06768 8
DUDLEY KNOX LIBRARY